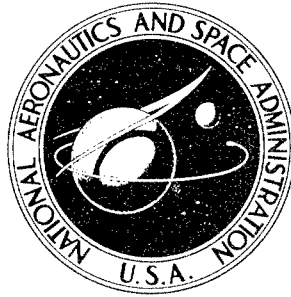


NASA CONTRACTOR
REPORT



012009
NASA CR-333

NASA CR-333

AMPTIAC

DISTRIBUTION STATEMENT A
Approved for Public Release
Distribution Unlimited

FATIGUE BEHAVIOR OF Ti-8Al-1Mo-1V SHEET
IN A SIMULATED WING STRUCTURE UNDER
THE ENVIRONMENT OF A SUPERSONIC TRANSPORT

by John J. Peterson

Prepared under Contract No. NAS 1-2998 by
LTV VOUGHT AERONAUTICS
Dallas, Texas
for Langley Research Center

20020319 104

NATIONAL AERONAUTICS AND SPACE ADMINISTRATION • WASHINGTON, D. C. • NOVEMBER 1965

FATIGUE BEHAVIOR OF Ti-8Al-1Mo-1V SHEET IN A SIMULATED
WING STRUCTURE UNDER THE ENVIRONMENT
OF A SUPERSONIC TRANSPORT

By John J. Peterson

Distribution of this report is provided in the interest of
information exchange. Responsibility for the contents
resides in the author or organization that prepared it.

Prepared under Contract No. NAS 1-2998 by
LTV VOUGHT AERONAUTICS
Dallas, Texas

for Langley Research Center

NATIONAL AERONAUTICS AND SPACE ADMINISTRATION

FATIGUE BEHAVIOR OF Ti-8Al-1Mo-1V SHEET
IN A SIMULATED WING STRUCTURE UNDER
THE ENVIRONMENT OF A SUPERSONIC TRANSPORT

By John J. Peterson
LTV Vought Aeronautics Division

SUMMARY

This report describes a test program conducted on realistic structural assemblies, to evaluate the fatigue behavior of a candidate material for use on the supersonic transport (SST) aircraft.

Tests were conducted on box-beams with tension skins simulating typical skin-stringer structures. The tension skin test specimens were fabricated from triplex annealed Ti-8Al-1Mo-1V. Tests were conducted under constant amplitude loading conditions at room temperature and at 550°F and spectrum tests were performed under conditions which simulated, as nearly as possible, the environment of the SST. A total of eight specimens were fabricated and tested during this investigation, four specimens employed spot-welds as the structural joining media and four used rivets. *copy → 16 of 17*

INTRODUCTION

In recent years LTV Vought Aeronautics Division has been actively engaged in research to investigate the fatigue characteristics of candidate materials for use on the supersonic transport airframe. The program which is reported herein represents one portion of this research effort. This research program was sponsored by the National Aeronautics and Space Administration under Contract NAS1-2998.

A particular problem in the development of the SST lies in the area of fatigue behavior of airframe materials when exposed to the operating environment of this vehicle. In order that the SST be economically feasible it will be necessary for the vehicle to have an extremely long service life. A large percentage of the flight time experienced by the SST will be spent in cruise at Mach 3 where the structure will be exposed to temperatures as high as 550°F. A relatively small amount of information is available on the fatigue behavior of structural materials at these temperatures and an even smaller store of knowledge is available concerning the performance of fabricated structures under these conditions.

The use of a box-beam incorporating various design problems which can be utilized for evaluating different construction techniques such as spot-welding, riveting and fusion welding is well suited to realistic evaluation of structural behavior.

In an effort to supplement the information now available and to gain an insight into the manner in which large structural components will react to the operating environment of the SST, a series of tests were conducted on box-beam specimens. The box-beams were designed with tension covers representative of typical wing skin structure suited for use on the SST. Only spotwelded and riveted constructions were included in this program although the design of the box-beam is equally suited for construction utilizing fusion welding.

SYMBOLS

C.A.	constant amplitude fatigue test
f	frequency of occurrence of flight load
GAG	ground-air-ground cycle, variation in load factor associated with the transfer of load from the landing gear to the wing and back to the landing gear
G.L.	test specimen gage length-inches
K_t	theoretical stress concentration factor
l_c	crack length-inches
L.F.	airplane load factor
R	stress ratio, the ratio of the minimum to the maximum stress in a load cycle
S_{tu}	ultimate tensile stress
S_{alt}	alternating stress in a fatigue cycle
S_{lgD}	stress level at take-off design gross weight
S_{mean}	the algebraic mean of the maximum and minimum stress in one cycle: $S_{mean} = (S_{max} + S_{min})/2$
S_{max}	the highest algebraic value of stress in the stress cycle with tensile stresses positive
S_{min}	the lowest algebraic value of stress in the stress cycle with tensile stresses positive

S_T thermal stress component, $0.65 \times S_{lg_D}$
 W^* ratio of instantaneous weight to take-off gross weight
 θ a non-dimensional parameter which expresses the ratio of the alternating stress component of a cycle to S_{lg_D}

SPECIMEN DESIGN

General.- A box-beam measuring 120 inches in length, 22.50 inches in width and 8.0 inches in depth was used as a test vehicle during this program. The box-beam consisted of two separate assemblies (1) a tension cover, which was used as a test specimen, simulating typical skin-stringer construction and (2) the remainder of the box-beam structure consisting of a compression cover, internal and external shear webs and bulkheads to stabilize the tension cover. The beams were designed to apply constant bending loads to the test section through the use of hydraulic actuators. Axles were employed to apply loads to the test structure in order to minimize the possibility of applying eccentric moments. The general arrangement of the box-beam is presented in Figure 1 and Figure 2 shows a completed box-beam installed in the test fixture.

Test Skins.- A total of eight tension skin test specimens were fabricated from triplex annealed Ti-3Al-1Mo-1V having a nominal thickness of 0.050 inch. This material was furnished by the National Aeronautics and Space Administration for use on this program.

The test specimens are conventional skin-stringer panels measuring 120 inches by 22.50 inches, these panels contain five channel section stiffeners running the length of the panel as shown in Figure 3. Typical stress raisers are incorporated in the 48 inch test section in the form of a small non-structural cut-out, a transverse skin splice at the center-line of the panel, and a large structural door. Figures 4, 5 and 6 are sketches showing pertinent details of construction in these areas.

Four panels were fabricated using rivets as the joining method, and four used spotwelds as the primary joining method. With the exception of the joining techniques utilized for beam fabrication all details of each type of test panel were identical.

Box Beam Fixtures.- Since the objective of this investigation was to evaluate the fatigue behavior of wing skin structures suited for use on the SST, a box-beam was considered the most suitable test article. In order that material usage and costs be held to a minimum, a reusable box-beam, see Figure 7, was designed so that failures in the tension skin would not precipitate a catastrophic failure in the primary box structure. A total of three box-beam structures of this type (box-beams minus tension skins, hereafter referred to as "basic boxes") were fabricated from annealed Ti-6Al-4V.

TEST FIXTURES AND EQUIPMENT

The test articles were loaded in test fixtures designed to impose constant moments over the length of the test section in accordance with the sketch of Figure 8. Elevated temperatures were attained through the use of a furnace which was large enough to enclose the entire box-beam assembly.

Test loads were applied to the specimen by a pair of 50 000 pound capacity servo controlled hydraulic actuators. Commands to the actuators were supplied by a closed loop electronic controller which has three separate control functions: (1) a 15 channel ramp generator which applies preset loads as commanded by a punched tape, (2) a controller which is a curve following device that generates a command signal as a function of its displacement, and (3) an oscillator which is used for the application of sine wave, square wave or sharp spike alternating loads. In operation, a feedback signal from a calibrated load ring in series with the actuator is compared with a command signal generated by the programming device. An imbalance in the two signals produces an additional command signal to the servos to load in the direction necessary to balance the system. An additional function of the control equipment is to determine the magnitude of this difference for error detection. Any difference greater than the preset allowable will shut the system down.

In a system of this type, it is not possible to attain an instantaneous reduction of load upon failure of the test specimen. In order to minimize damage to the reusable box-beam in the event of a catastrophic failure of the tension skin, physical stops were incorporated in the test fixture to prevent excessive deflection during the time interval when the load was dropping off.

Photographs showing the furnace and control equipment are presented in Figures 9 and 10.

MATERIALS

One candidate material was selected for evaluation on this program. This material was Ti-8Al-1Mo-1V in the triplex annealed condition. This material was furnished by the National Aeronautics and Space Administration for use on this program and had the following chemical composition and processing history:

Chemical Composition.

<u>Element</u>	<u>Percent</u>
Carbon	0.023
Iron	0.09
Nitrogen	0.013
Aluminum	7.60
Vanadium	1.00
Molybdenum	1.10
Hydrogen	0.003 - 0.014
Titanium	Balance

Mechanical Properties Reported by Mill.

	Min	Max	Avg
S _{tu}	142 300	152 600	147 000
S _{ty}	130 300	141 100	133 000
Elongation %	11	13	11

Mechanical Properties Determined by LTV. - Tests were conducted on "as received" material at LTV prior to specimen fabrication, the resulting properties were as shown below:

Room Temperature

				Avg
S _{tu}	151 700	152 500	152 400	152 200
S _{ty}	132 500	133 600	135 400	133 800
Elongation %	13.2	14.4	13.4	13.7

550°F, 1/2 Hour Soak

				Avg
S _{tu}	124 100	125 200	125 900	125 100
S _{ty}	98 500	100 000	99 600	99 300
Elongation %	10.2	9.9	9.7	9.9

1
5 →
p-20

Processing History.

1. Rolling temperature from roughdown to finish sheet, approximately 1800°F.
2. Sheets resquared and chemically descaled.
3. Annealed in car-bottom furnace at 1450°F, 8 hours, slow cool to below 800°F, air cool; reanneal at 1850°F, 5 minutes, air cool; condition and final anneal at 1375°F for 15 minutes and air cool.
4. Final finish by pickle and grind sequence.

TEST CONDITIONS

Spectrum.- A loading schedule which is considered representative of service conditions on the wing of the SST was selected for use on this program with the approval of the NASA technical monitor. This spectrum contains GAG loads, gust and maneuver loads, loads occurring during check flights, and loads due to thermal stresses. Loads are presented for the climb and cruise portions of the mission profile only since the loads to be experienced during let-down are below the endurance limit of the material being used.

The basic spectrum for this program is presented in Table I. The spectrum, as shown, is representative of the loads to be experienced during approximately 30 000 hours of flying time and contains loads for 12 000 operational flights plus 500 check flights.

During spectrum tests, the mean stresses applied to the specimen were varied to reflect the changes in airplane gross weight which occur during a flight. The relative value of the mean (or lg) stress level is defined by W^* which is the ratio of instantaneous weight to the take-off gross weight. Since $S_{lgD} = 25\ 000$ psi, the nominal mean stress at any time is $(W^*)(25\ 000)$.

The values of W^* used for these tests were:

- a. Take-off and climbs, $W^* = 1.0$
- b. Cruise, $W^* = 0.75$
- c. Check flights, $W^* = 0.70$

Since the spectrum is defined in terms of θ , the maximum stress in any cycle may be obtained using the following relationship:

$$S_{\max} = S_{\text{mean}} + S_{\text{alt}} = (S_{lgD})(W^* + \theta) \text{ for take-off, climb and check flight loads.}$$

Since the test set-up was designed to minimize thermal stresses, the mean stress used during the cruise portion of the flight was increased by an amount equal to $(0.65)(S_{lg_D})$ to simulate thermal stresses. For the cruise portion of the spectrum test the maximum stress may then be defined as:

$$S_{max} = (S_{lg_D})(W* + \theta + 0.65) = (S_{lg_D})(1.40 + \theta)$$

In order to attain maximum realism in a test of this type, all loads and heating cycles should be simulated on a flight by flight basis. This was impractical because of the excessive amount of time required for temperature cycling. In view of this problem a block containing two percent of the total spectrum life (240 operational flights plus 10 check flights) was selected as the best compromise.

Since the possibility of either gust or maneuver loads occurring during the heated portion of the climb profile is negligible, GAG, climb and check flight loads were applied at ambient temperature and cruise loads were put on at 550°F.

All ambient temperature loads were applied on a flight by flight basis in order to simulate, as closely as possible, the actual order of load application on the full scale structure. Cruise loads (550°F) were applied in the form of a random block which contained the loads for all 240 operational flights. Loads occurring less than once per block were applied in randomly selected blocks during the course of the test.

Tables II, III, and IV show a breakdown of the manner in which spectrum loads were applied to the test specimens.

Table II specifies the number of load cycles which were applied to the test specimens on a flight by flight basis including those for check flights. These loads were applied at ambient temperature during each block of testing.

Table III presents the load cycles applied to the specimen during the heated (cruise) portion of each block.

Load cycles whose frequency of occurrence was such that they could not be included in either segment of the basic block as described in the preceding paragraphs were applied in randomly selected blocks in accordance with the information contained in Table IV. Wherever applicable these loads were inserted in randomly selected flights within the block.

Constant Amplitude.- Constant amplitude tests were conducted as a means of establishing correlation with available simple element fatigue data and to establish the basic fatigue characteristics of the test specimens.

Since the GAG cycle is normally expected to produce a major portion of

the fatigue damage felt by the structure one specimen of each configuration was tested at room temperature under GAG loads ($S_{max} = 25$ ksi, $S_{min} = -12.5$ ksi).

In order that the behavior of the test structure might be observed under loads incurred at elevated temperature, one specimen of each configuration was tested under constant amplitude loading conditions at 550°F. These specimens were tested under the cruise loading condition having the highest frequency of occurrence ($S_{max} = 41.25$ ksi, $S_{min} = 28.75$ ksi).

TEST PLAN

A total of eight specimens were tested during the course of this investigation, four spotwelded and four riveted. The specimens were tested in accordance with the following table:

Panel Number	Type of Construction	Test Condition
1	Spotwelded	Spectrum test
2	Spotwelded	C.A., RT GAG loads (1)
3	Spotwelded	C.A., 550°F, Cruise loads (2)
4	Spotwelded	Spectrum
5	Riveted	C.A., RT GAG loads (1)
6	Riveted	Spectrum
7	Riveted	C.A., 550°F, Cruise loads (2)
8	Riveted	Spectrum

(1) $S_{max} = 25\ 000$ psi, $S_{min} = -12\ 500$ psi

(2) Test conducted at 35 000 psi \pm 6250 psi

Prior to testing the first specimen, a proof load to the lg load level was conducted to obtain strain information from strain gages and photoelastic coatings.

The lg stress level at take-off was assumed to be 25 000 psi tension. The load factors used for design of the test specimens were in accordance with Civil Air Regulations - Part 4b with one exception. Since the only material thickness available for fabrication of the test specimens was 0.050 inch, it was not possible to keep the skins non-buckling to a negative load factor of 1.0g without using excessively small stiffener spacing. Therefore the panels were designed to be non-buckling only to the lowest load level to be encountered during the course of testing. This load

level was -0.50g, or 12 500 psi compression.

PROOF LOAD TEST

General.- Prior to testing, spotwelded test skin number 1 was completely instrumented with photostress plastic and strain gages to be used in establishing strain distributions. Proof loads were applied to the specimen in 5000 lb. increments up to the load estimated to produce nominal skin stresses of 25 000 psi (this load was 20 000 lbs). Permanent records were made of strain gage readings and photostress fringes.

Summary of Results. - Figures 11, 12, and 13 are photographs showing isochromatics observed in the critical areas of the test section. Figure 14 shows measured stress levels at various locations within the test section at an applied load of 20 000 lbs. Figure 15 shows the location of strain gages within the test section while observed strain values at the incremental load points are shown in Table V.

As reported earlier, the test panels were designed to be non-buckling only to the lowest stress level to be reached during this program. During proof loading to a stress level of -12 500 psi, many compression buckles were observed in the test section. These buckles were found in all areas not backed up by doublers and occurred at relatively low load levels. Thickness measurements made on this and all other test specimens revealed that the thickness of the Ti-8Al-1Mo-1V used for specimen fabrication varied considerably from the nominal value of 0.050 which was used for design purposes. These measurements showed that there were some areas in the specimens as thin as 0.039 and, further, that in very few instances were measurements as high as 0.050 recorded. Table VI presents the results of this thickness survey.

Further checking gave evidence that the compression buckles were not permanent in nature and, since a "fix" was considered impractical, testing was continued as planned. Whenever possible those specimens having minimum thickness in the critical buckling areas were tested under conditions where buckling was not critical.

REPEATED LOAD TESTS

General.- A fatigue failure is usually defined as rupture of a component due to the application of repeated loads, none of which are of sufficient magnitude to produce a failure when acting alone. In most tests conducted on small specimens this approach is generally used to define failure. This criteria is generally unsatisfactory for tests conducted on large, complex, thin skin-stringer type structures such as tested in this program since the interval between detection of a crack and actual failure of the article may encompass the applications of many additional cycles of

load and result in growth of cracks to several inches in length. For the purposes of this report, crack initiation is defined as the point when a crack has a length of 0.03 inch and the structure is considered to be no longer suitable when at least one crack has attained a length of 0.50 inch. The majority of tests conducted on this program were carried to a point beyond a crack length of 0.50 inch in order to generate additional data on the crack propagation characteristics of the program material.

Summary of Results.- The following table presents a brief summary of the results of all tests conducted during this investigation.

Spec. No.	Type Test	S _{max} psi	Predicted Life	Time to lc = .03 in	Time to lc = .50 in	Test Stopped
1 S/W	Spect	53 750	3 100 flts	(1)	--	--
4 S/W	Spect	53 750	3 100 flts	775 flts(3)	1 000 flts(3)	2 500 flts
6 Riv	Spect	53 750	7 400 flts	5 600 flts	6 815 flts	12 500 flts
8 Riv	Spect	53 750	7 400 flts	9 500 flts	(2)	12 500 flts
2 S/W	C.A.	25 000	13 000 cyc	--	25 000 cyc(3)	33 345 cyc
5 Riv	C.A.	25 000	36 000 cyc	8 450 cyc	24 000 cyc	48 301 cyc
3 S/W	C.A.	41 250	75 000 cyc	49 400 cyc	80 750 cyc	159 955 cyc
7 Riv	C.A.	41 250	90 000 cyc	41 700 cyc	99 000 cyc	154 047 cyc

1. This specimen experienced an instability failure after completion of 1250 flights.
2. Cracks had not attained length of 0.50 inch after completion of 12 500 flights.
3. Based on extrapolation of test data.

Description of Failures.- In all specimens (with the exception of number 1) the presence of widespread fatigue cracking was confined to the critical design areas: i.e. the center splice, the structural door, and the circular cutout. The critical sections of the test section listed in the order of relative severity are (1) the end attachments in the large structural door doubler, (2) the first row of attachments between the skin and bearing doubler at the centerline splice and, (3) the ends of the doubler reinforcing the small circular cutout. All fatigue cracks were confined to the skin only and, in addition, were usually found in the vicinity of loaded attachments. Of 201 observed fatigue cracks only 6 were found adjacent to non-loaded attachments. Figure 16 shows typical fatigue cracks in the vicinity of spotwelds and rivets.

Spotwelded Test Specimen Number 1

This specimen was tested under spectrum loading conditions. Following completion of five blocks of spectrum loading, 1250 flights, the test skin suffered a catastrophic instability failure. Subsequent investigation indicated that a slight overload coupled with the effects of under tolerance titanium sheet (see page 9) material was responsible for the failure. At the time of failure there were no indications of fatigue damage anywhere in the specimen.

Spotwelded Test Specimen Number 2

Specimen number 2 was tested at room temperature under GAG loads, $S_{\max} = 25$ ksi and $S_{\min} = -12.5$ ksi. Cracks were not observed in this specimen until after 31 344 cycles of load had been applied. At this time a total of 38 cracks were recorded. The lengths of these cracks varied from 0.10 inch to 1.37 inch. From the length of some of these cracks, it was apparent that they had been present for a considerable time without being detected during normal inspections. After the completion of 33 345 loading cycles some of the cracks had grown to a length sufficient to warrant discontinuation of the test.

A copy of the inspection log for this specimen is shown in Table VII and Figure 17 shows the location of the fatigue cracks observed during the test. Crack propagation curves are shown in Figure 24.

Although it was not possible to obtain an accurate estimate of the time at which a crack length of 0.03 inch was attained, a reasonable estimate of the time to reach a crack length of 0.50 inch was obtained from the crack growth data available for this specimen. This time was 25 000 cycles.

Spotwelded Test Specimen Number 3

This specimen was tested under constant amplitude loading at 550°F with $S_{\max} = 41.25$ ksi and $S_{\min} = 28.75$ ksi. A crack length of 0.03 inches was reached after 49 400 cycles of load and a length of 0.50 inch was reached after 80 750 cycles. Testing was discontinued after a total of 159 955 cycles at which time the specimen contained a total of 12 actual fatigue cracks and 2 potential fatigue crack nuclei.

A copy of the inspection log is presented as Table VIII. The locations of all fatigue cracks are shown in Figure 18 while crack propagation curves for selected cracks are shown in Figure 25.

Spotwelded Test Specimen Number 4

This specimen was tested under spectrum loading conditions with $S_{lgD} = 25$ ksi. After 3 spectrum blocks (750 flights) had been applied to the specimen prominent areas of strain deformation were observed adjacent to 19 spotwelds in the door doubler and centerline splice areas of the test section. These incipient crack locations were logged and the test was continued. Upon completion of 1250 flights, cracks up to 0.60 inch long were observed in the majority of those areas which showed initial strain markings. Upon completion of 2500 flights cracking was sufficiently widespread to stop testing. At this time 64 cracks with lengths up to 6.0 inches had been logged. Table IX shows the inspection log for this test, Figure 19 locates all cracks and Figure 26 presents propagation data for selected cracks in critical areas.

Riveted Test Specimen Number 5

This specimen was tested at room temperature under GAG loading with $S_{max} = 25$ ksi and $S_{min} = -12.5$ ksi. Initial cracking was observed after 8450 cycles of load. A crack length of 0.50 inch was attained upon completion of 24 000 cycles. Testing was stopped after 48 301 load cycles had been applied to the specimen at which time 14 cracks had been observed in the test section. At this time the total crack length in the critical section of the specimen was approximately 14 inches which represents 30 percent of the total tension area.

Table X shows the inspection log for this specimen, and Figures 20 and 27 show the location of fatigue cracks and crack propagation information obtained from this test.

Riveted Test Specimen Number 6

Test specimen number 6 was tested under spectrum loading conditions with $S_{lgD} = 25$ ksi. Initial cracking was detected after the completion of 5600 flights. Upon completion of 6815 simulated flights a crack had grown to a length of 0.50 inch. Cycling was continued until 12 500 flights had been completed at which time the test was stopped. At this time, the specimen contained a total of 17 cracks with lengths varying up to approximately 3.50 inches.

The inspection log for this specimen is shown in Table XI, crack locations and crack propagation curves are presented in Figures 21 and 28 respectively.

Riveted Test Specimen Number 7

This specimen was tested under constant amplitude conditions at 550°F, $S_{\max} = 41.25$ ksi and $S_{\min} = 28.75$ ksi. Initial cracking ($l_c = 0.03$) was observed in the test skin at the end of the door doubler following the application of 41 700 load cycles. This crack had grown to a length of 0.50 inch after 99 000 cycles. Testing was terminated after 154 047 cycles at which time the specimen contained 47 cracks with lengths ranging up to approximately 3.0 inches.

The inspection log for this specimen is shown in Table XII, crack locations and crack propagation curves are shown in Figures 22 and 29 respectively.

Riveted Test Specimen Number 8

The number 8 specimen was tested under spectrum loading conditions with $S_{lgD} = 25$ ksi. At the completion of 9500 simulated flights a crack length of 0.03 inch was reached. The test was continued until 12 500 flights had been applied. At this time the specimen contained 3 small cracks in the test section with a maximum observed length of 0.10 inch.

The inspection log for this specimen is shown in Table XIII and Figure 23 is a sketch showing the location of the observed cracks. Crack propagation curves for this specimen are presented in Figure 30.

FATIGUE ANALYSIS

Fatigue analyses were conducted on both specimen configurations for comparison with test results. The data used for these analyses were:

1. Fatigue data for non-load carrying spotwelds and load carrying bolted joints as contained in reference (1).
2. S-N data for notched ($K_t = 4.0$) specimens as presented in reference (2).
3. Test information for load carrying spotwelded joints as presented in Appendix A to this report.

Fatigue life predictions which were obtained using the above data were as shown in the following table:

Spec. Type	Test Cond	Predicted Life		
		Reference (1)	Reference (2)	Appendix A
S/W	Spectrum	2.35×10^4 flts		3.1×10^3 flts
S/W	C.A., GAG	10^5 cyc		1.3×10^4 cyc
S/W	C.A., 550°F	10^6 cyc		7.5×10^4 cyc
Riv	Spectrum	4.65×10^4 flts	7.4×10^3 flts	
Riv	C.A., GAG	10^5 cyc	3.6×10^4 cyc	
Riv	C.A., 550°F	2×10^5 cyc	9×10^4 cyc	

Since the fatigue data in reference (1) were for non-load carrying spotwelds and were not truly representative of the test specimens used during this program, fatigue data for load carrying spotwelds as reported in Appendix A was generated for comparison purposes. As shown in the preceding table, the fatigue lives predicted for spotwelded specimens using reference (1) data were from 7 to 13 times higher than those using the data in Appendix A. In addition, the data contained in Appendix A furnished better correlation with the observed test results.

Predicted fatigue lives for the riveted test specimens based on the bolted joint data contained in reference (1) were as much as 4 times higher than those observed during this investigation. These data were for a protruding head bolted joint with an apparent K_t of approximately 2.5 and, as such, were not adequate for estimating the behavior of the countersunk riveted and/or bolted connections used on this specimen. Use of the notched ($K_t = 4.0$) fatigue data contained in reference (2) for estimating fatigue lives resulted in improved correlation with the observed fatigue lives of these specimens and indicated that, for the type of construction used in this program, the apparent stress concentration was at least as high as 4.0.

DISCUSSION

Constant Amplitude Tests.- The spotwelded and riveted specimens showed similar fatigue lives based on a crack length of 0.5 inch, but the number of cracks observed, the rates at which they propagated and the times at which they formed differed widely.

Reasonable estimates of fatigue life were obtained through the use of simple element fatigue data of reference (2) and Appendix A. Use of the data of reference (1) for unloaded spotwelds and bolted joints resulted in predicted lives well in excess of test results.

For both tests conditions and specimen types, cracks appeared in the same general locations and in the same relative order. Cracks were observed first at the ends of the large door doubler followed by cracking at the first row of attachments in the centerline splice doubler and then cracking in the skin at the ends of the doubler around the circular cut-out.

Spectrum Tests. - The agreement in fatigue lives between spotwelded and riveted test specimens observed during constant amplitude testing did not exist during spectrum testing. As in the constant amplitude tests, the number of cracks observed, the propagation rates and times at which they formed differed widely.

Fatigue life predictions based on the data contained in reference (1) for unloaded spotwelds and bolted joints, were well in excess of the experimental lives obtained during testing. The data contained in reference (2) for $K_t = 4.0$, and Appendix A to this report for loaded spotwelds, furnished improved correlation with these test results. However, the linear cumulative damage theory overestimated the fatigue lives of both spotwelded specimen number 4 and riveted specimen number 6, while riveted specimen number 8 demonstrated a fatigue life at least 25 percent higher than predicted.

The location of cracks in the test section and the general order of their initiation were the same as observed during constant amplitude testing.

Fatigue Crack Behavior. - As previously noted, the location and relative order of appearance of cracks was the same for all tests.

At the time that crack lengths of 0.50 inch were attained, the spotwelded specimens were seen to contain approximately 3 times more cracks than the riveted specimens. However, at the conclusion of testing the total number of cracks observed in each specimen could not be related to either test condition or specimen configuration.

Determination of the first crack to form was not possible in all cases but, with the exception of test specimen number 6, the first crack to attain a length of 0.50 inch was in the first group of cracks found during inspection. As shown in the inspection log for test specimen number 6 (Table XI) the first crack to grow to a length of 0.50 inch was in the second group of cracks rather than the first but, as in the other tests, this crack was located through the end attachments of the large structural door doubler.

Crack growth patterns for those cracks which propagated through the test were similar in both specimen types. Initial growth was at a fairly uniform rate until a length from 0.25 to 0.50 inch was attained at which time an increase in rate was observed. Although the general shape of the crack growth curves are similar for both specimen configurations, the rate of propagation varies widely. When the growth rates for identically located spotwelds and rivets were compared, it was seen that the rate in spotwelded specimens was from 1.5 to 4 times the rate observed in riveted

specimens.

Comparison of Constant Amplitude and Spectrum Tests. - A comparison of the test results obtained during this program was made by assuming that the experimental and calculated fatigue lives under both spectrum and constant amplitude loading conditions would be related in the same manner.

The calculated spectrum life which was established through the use of the linear cumulative damage theory and the S-N data for simple specimens reported in reference (2) and Appendix A, was multiplied by the ratio of the box beam constant amplitude life to the constant amplitude life of the simple specimens to obtain a corrected life prediction. This predicted life was then compared to the observed test life under spectrum loading conditions.

The results of this comparison are presented in Table XIV. It can be seen from this table that, for the limited data available, there was no consistent relationship between the constant amplitude and spectrum fatigue tests.

CONCLUSIONS

1. The box beams used during this program provided a reasonable vehicle for supplying data on the fatigue behavior of Ti-8Al-1Mo-1V sheet material when fabricated into structures suited for use on the SST.
2. Fatigue data contained in reference (2) for notched ($K_t = 4.0$) specimens and in Appendix A for load carrying spotwelded specimens was in good agreement with the results obtained during constant amplitude testing.
3. The linear cumulative damage theory, applying constant amplitude test data in analysis, did not provide realistic estimates for spectrum fatigue life.
4. When tested under spectrum loading conditions the spotwelded and riveted specimens demonstrated fatigue lives which were not related.
5. Both spotwelded and riveted specimens had approximately equal lives to $lc = 0.50$ inches during constant amplitude testing. Initial cracking and crack growth rates were not related.

6. The location of cracks and their order of appearance were not influenced by the type of test or by the specimen configuration. The constant amplitude tests were adequate for the determination of critical areas within the specimen.
7. The spotwelded specimens contained three times the number of cracks seen in the riveted specimens at the time $t_c = 0.50$ inch.
8. The cracks which were the first to reach a length of 0.50 inch were among the first to form and were located at the end attachments of the large structural door doubler.
9. Crack ^{Ti}propagation rates in the spotwelded test specimens were as much as four times the rate seen when testing riveted specimens.
10. The Ti-8Al-1Mo-1V skin-stringer test panels used during this program did not suffer catastrophic failures in the presence of fatigue cracks which eliminated as much as 30 percent of the net tension area. |

← pg 5

APPENDIX A

TESTS TO DETERMINE THE FATIGUE CHARACTERISTICS OF LOAD CARRYING SPOTWELDS

In any practical structure, the majority of the fasteners which are used in assembly will be loaded to some degree and this is true of the specimens which were tested during this investigation. Since the simple element fatigue data reported in reference (1) were for spotwelds in which no load transfer was involved, and which were therefore representative of the best behavior to be attained using spotwelds, it was not possible to obtain satisfactory correlation with the tests conducted during this investigation.

In order to obtain a better insight into the performance of load carrying spotwelds, and to provide a more realistic basis for comparison, a group of spotwelded specimens were fabricated at LTV and tested by NASA. Specimen geometrics were selected to simulate, as closely as possible, the stress and load distributions observed through the use of photoelastic coatings applied to the critical areas of a spotwelded test specimen. The specimens used for these tests are presented in Figure 31.

Constant amplitude fatigue tests were conducted at room temperature and 550°F under a constant mean stress of 25 ksi in order to be consistent with the data contained in reference (1). As a further check into the behavior of these load carrying spotwelds, a group of specimens was also tested to the G.A.G. load cycle ($S_{\max} = 25$ ksi, $S_{\min} = -12.5$ ksi).

The results of these tests were used to construct modified Goodman diagrams in the manner described in reference (1).

Test results are presented in Table XV and the modified Goodman diagrams constructed from this data are shown in Figure 32.

55866

(REFERENCES)

1. Peterson, J. J.: Fatigue Behavior of AM-350 Stainless Steel and Titanium 8Al-1Mo-1V Sheet at Room Temperature, 550°F and 800°F. NASA CR-23, May 1965
2. Gideon, D. N.; Marschall, C. W.; Holden, F. C.; and Hyler, W. S.; Exploratory Studies of Mechanical Cycling Fatigue Behavior of Materials for the Supersonic Transport. NASA CR 28, April 1964

— end

TABLE I

CUMULATIVE FREQUENCIES OF COMBINED GUST
AND MANEUVER LOADS

(12000 Operational Flights and 500 check Flights)

θ	Climb		Cruise		Check Flt.	
	Total	Block	Total	Block	Total	Block
0.25	78 000.0	1 560.00	3000.0	60.00	11,500.0	230.00
0.35	13 200.0	264.00	552.0	11.04	2 800.0	56.00
0.45	3 120.0	62.40	84.0	1.68	1 000.0	20.00
0.55	670.0	13.40	8.4	0.17	300.0	6.00
0.65	145.0	2.90			75.0	1.50
0.75	40.0	0.80			15.0	0.30
0.85	18.0	0.36				
0.95	9.0	0.18				
1.05	4.0	0.08				
1.15	2.5	0.05				
G.A.G.	12 000.0	240.00			3 500.0	70.00

Notes:

1. G.A.G. cycle for operational flights varies from $-0.5 S_{1g_D}$ to $+ 1.0 S_{1g_D}$
2. G.A.G. cycle for check flights varies from $-0.5 S_{1g_D}$ to $+0.7 S_{1g_D}$
3. Mean stress for climb loads = $(1.0)(S_{1g_D})$
4. Mean stress for cruise loads = $(0.75)(S_{1g_D}) + (0.65)(S_{1g_D})$
5. Mean stress for check flights = $(0.70)(S_{1g_D})$
6. θ defines the alternating stress component of load:
 $\epsilon_{alt} = \theta S_{1g_D}$
7. $S_{1g_D} = 25\ 000$ psi.
8. Loads incurred during descent not included, below endurance limit.

TABLE II

FATIGUE SPECTRUM-BASIC RT BLOCK
 240 Operational + 10 Check Flights
 Climb + Gag Loads

Flight No.	$\theta = 25$	$\theta = 35$	$\theta = 45$	$\theta = 55$	$\theta = 65$	GAG	W*
1	6	1	1			1	1.0
2	7	1				1	1.0
3	6	1	1			1	1.0
4	7	1				1	1.0
5	7	1				1	1.0
6	6	1				1	1.0
7	6	1				1	1.0
8	7	1				1	1.0
9	7	1	1			1	1.0
10	7	1				1	1.0
11	7	1				1	1.0
12	6	1				1	1.0
13	6	1				1	1.0
14	7	1				1	1.0
15	7	1				1	1.0
16	6	1	1			1	1.0
17	6	1				1	1.0
18	7	1		1		1	1.0
19	7	1				1	1.0
20	7	1	1			1	1.0
21	7	1		1		1	1.0
22	7	1	1			1	1.0
23	6	1				1	1.0
24	7	1				1	1.0
Check#1	23	6	2		1	7	0.7
26	7	1				1	1.0
27	7	1				1	1.0
28	6	1	1			1	1.0
29	7	2				1	1.0
30	6	1				1	1.0
31	6	1				1	1.0
32	7	1	1			1	1.0
33	6	1				1	1.0
34	6	1				1	1.0
35	6	1				1	1.0
36	7	1				1	1.0

TABLE II (Cont'd)

FATIGUE SPECTRUM-BASIC RT BLOCK
 240 Operational+10 Check Flights
 Climb and Gag Loads

Flight No.	$\theta = 25$	$\theta = 35$	$\theta = 45$	$\theta = 55$	$\theta = 65$	GAG	W*
37	7	1				1	1.0
38	7	1				1	1.0
39	6	1				1	1.0
40	6	1				1	1.0
41	7	1	1			1	1.0
42	7	1				1	1.0
43	6	1				1	1.0
44	6	1				1	1.0
45	7	1				1	1.0
46	6	1				1	1.0
47	7	1				1	1.0
48	6	2				1	1.0
49	7	1			1	1	1.0
Check #2	23	6	2	1		7	0.7
51	7	1				1	1.0
52	6	1				1	1.0
53	7	1				1	1.0
54	7	1				1	1.0
55	6	2	1			1	1.0
56	6	1				1	1.0
57	7	1				1	1.0
58	6	2	1			1	1.0
59	7	1				1	1.0
60	6	1				1	1.0
61	7	1	1			1	1.0
62	6	2				1	1.0
63	6	2	1			1	1.0
64	7	2				1	1.0
65	6	1				1	1.0
66	6	1				1	1.0
67	7	1	1	1		1	1.0
68	6	1	1			1	1.0
69	7	1	1			1	1.0
70	6	1				1	1.0
71	6	1				1	1.0
72	7	1	1			1	1.0

TABLE II (Cont'd)

FATIGUE SPECTRUM-BASIC RT BLOCK
 240 Operational + 10 Check Flights
 Climb and Gag Loads

Flight No.	$\theta = 25$	$\theta = 35$	$\theta = 45$	$\theta = 55$	$\theta = 65$	GAG	W*
73	6	1	1			1	1.0
74	7	1	1			1	1.0
Check #3	23	5	2		1	7	0.7
76	7	1				1	1.0
77	6	1	1			1	1.0
78	6	1	1			1	1.0
79	7	1				1	1.0
80	6	2		1		1	1.0
81	6	1	1			1	1.0
82	7	2	1			1	1.0
83	6	1	1			1	1.0
84	7	1	1			1	1.0
85	7	1				1	1.0
86	6	2	1			1	1.0
87	7	1	1			1	1.0
88	6	1				1	1.0
89	6	1				1	1.0
90	7	1				1	1.0
91	6	1				1	1.0
92	7	1				1	1.0
93	7	2				1	1.0
94	6	1	1			1	1.0
95	7	1				1	1.0
96	6	1	1			1	1.0
97	6	1				1	1.0
98	7	1				1	1.0
99	6	1	1			1	1.0
Check #4	23	5	2	1		7	0.7
101	7	1				1	1.0
102	6	1				1	1.0
103	7	2				1	1.0
104	6	1	1			1	1.0
105	7	1				1	1.0
106	6	1				1	1.0
107	6	1	1			1	1.0
108	7	1				1	1.0

TABLE II (Cont'd)

FATIGUE SPECTRUM-BASIC RT BLOCK
 240 Operational+10 Check Flights
 Climb and Gag Loads

Flight No.	$\theta = 25$	$\theta = 35$	$\theta = 45$	$\theta = 55$	$\theta = 65$	GAG	W*
109	7	1				1	1.0
110	6	1				1	1.0
111	7	1				1	1.0
112	6	1				1	1.0
113	7	1				1	1.0
114	6	1				1	1.0
115	6	1				1	1.0
116	7	1	1			1	1.0
117	6	1				1	1.0
118	6	1				1	1.0
119	7	1	1	1		1	1.0
120	6	1				1	1.0
121	6	1				1	1.0
122	7	1				1	1.0
123	7	1				1	1.0
124	6	1	1	1		1	1.0
Check#5	23	5	2	1		7	0.7
126	6	1				1	1.0
127	7	1				1	1.0
128	6	1				1	1.0
129	7	2				1	1.0
130	7	2				1	1.0
131	6	1				1	1.0
132	6	1	1			1	1.0
133	7	1	1			1	1.0
134	7	1				1	1.0
135	7	2				1	1.0
136	7	1	1			1	1.0
137	6	1				1	1.0
138	6	1		1		1	1.0
139	7	1	1	1		1	1.0
140	7	1		1		1	1.0
141	6	1				1	1.0
142	6	2				1	1.0
143	7	1				1	1.0
144	7	1	1			1	1.0

TABLE II (Cont'd)

FATIGUE SPECTRUM-BASIC RT BLOCK
 240 Operational + 10 Check Flights
 Climb and Gag Loads

Flight No.	$\theta = 25$	$\theta = 35$	$\theta = 45$	$\theta = 55$	$\theta = 65$	GAG	W*
145	7	1				1	1.0
146	7	1				1	1.0
147	7	1				1	1.0
148	6	1	1			1	1.0
149	7	1				1	1.0
Check #6	23	6	2			7	0.7
151	7	1				1	1.0
152	7	1	1			1	1.0
153	6	1	1			1	1.0
154	7	1	1			1	1.0
155	6	1				1	1.0
156	6	1				1	1.0
157	7	1				1	1.0
158	6	1				1	1.0
159	6	1				1	1.0
160	6	1				1	1.0
161	7	1	1			1	1.0
162	7	1				1	1.0
163	7	1		1		1	1.0
164	6	1	1			1	1.0
165	6	1				1	1.0
166	7	1		1		1	1.0
167	7	1				1	1.0
168	6	2				1	1.0
169	6	1				1	1.0
170	7	1				1	1.0
171	6	2				1	1.0
172	7	1				1	1.0
173	6	1	1			1	1.0
174	7	1				1	1.0
Check #7	23	6	2	1		7	0.7
176	7	1				1	1.0
177	6	1				1	1.0
178	7	1				1	1.0
179	7	1				1	1.0
180	6	1				1	1.0

TABLE II (Cont'd)

FATIGUE SPECTRUM-BASIC RT BLOCK
 240 Operational + 10 Check Flights
 Climb and Gag Loads

Flight No.	$\theta = 25$	$\theta = 35$	$\theta = 45$	$\theta = 55$	$\theta = 65$	GAG	W*
181	6	1	1			1	1.0
182	7	1				1	1.0
183	6	1				1	1.0
184	7	1	1			1	1.0
185	6	1				1	1.0
186	7	1				1	1.0
187	6	1	1			1	1.0
188	6	1				1	1.0
189	7	1				1	1.0
190	6	1				1	1.0
191	6	1				1	1.0
192	7	1		1		1	1.0
193	6	1				1	1.0
194	7	1				1	1.0
195	6	1	1			1	1.0
196	6	1				1	1.0
197	7	1	1			1	1.0
198	6	2				1	1.0
199	7	1				1	1.0
Check#8	23	6	2	1		7	0.7
201	7	2	1			1	1.0
202	6	1				1	1.0
203	6	1	1			1	1.0
204	7	1				1	1.0
205	6	1	1			1	1.0
206	6	1				1	1.0
207	7	1				1	1.0
208	6	1				1	1.0
209	7	1	1			1	1.0
210	7	1				1	1.0
211	6	1				1	1.0
212	7	1				1	1.0
213	6	1				1	1.0
214	6	1				1	1.0
215	7	1				1	1.0
216	6	1	1	1		1	1.0

TABLE II (Concluded)

FATIGUE SPECTRUM-BASIC RT BLOCK
 240 Operational+ 10 Check Flights
 Climb and Gag Loads

Flight No.	$\theta = 25$	$\theta = 35$	$\theta = 45$	$\theta = 55$	$\theta = 65$	GAG	W*
217	7	1	1			1	1.0
218	7	1				1	1.0
219	6	1	1			1	1.0
220	7	1	1			1	1.0
221	6	1				1	1.0
222	6	1				1	1.0
223	7	2				1	1.0
224	6	1				1	1.0
Check #9	23	6	2			7	0.7
226	7	1				1	1.0
227	6	1				1	1.0
228	7	2				1	1.0
229	6	1				1	1.0
230	7	1				1	1.0
231	6	1				1	1.0
232	6	1				1	1.0
233	7	2				1	1.0
234	7	2				1	1.0
235	6	1				1	1.0
236	7	1				1	1.0
237	6	1				1	1.0
238	7	1				1	1.0
239	6	1				1	1.0
240	6	1				1	1.0
241	7	1				1	1.0
242	6	1				1	1.0
243	6	1				1	1.0
244	7	1				1	1.0
245	6	1	1			1	1.0
246	6	1	1			1	1.0
247	7	1				1	1.0
248	7	1				1	1.0
249	6	1				1	1.0
Check #10	23	5	2	1		7	0.7

TABLE III

FATIGUE SPECTRUM-BASIC 550°F BLOCK
 240 Operational Flights
 Cruise Loads

Load No.	$\theta = .25$	$\theta = .35$	$\theta = .45$	Load No.	$\theta = .25$	$\theta = .35$	$\theta = .45$
1	1			37	1		
2	1			38		1	
3	1			39		1	
4	1			40	1		
5	1			41	1		
6		1		42	1		
7	1			43	1		
8	1			44	1		
9	1			45	1		
10	1			46			1
11	1			47	1		
12	1			48	1		
13	1			49		1	
14	1			50	1		
15	1			51	1		
16	1			52		1	
17	1			53	1		
18	1			54	1		
19	1			55	1		
20	1			56	1		
21	1			57	1		
22	1			58	1		
23	1			59		1	
24	1			60	1		
25	1			61	1		
26		1		62	1		
27		1		63	1		
28	1			64	1		
29	1			65	1	1	
30	1			66	1		
31	1			67	1		
32	1			68		1	
33	1			69		1	
34	1			70	1		
35	1			71	1		
36	1			72	1		

TABLE IV

FATIGUE SPECTRUM-ADDITIONAL LOADS
(Not Included in Basic Block)

BLOCK	θ ITEM	.35	.45	.55	.65	.75	.85	.95	1.05	1.15
		1	Climb Check Cruise	No Change No Change No Change						
2	Climb Check Cruise			1	1	1	1			
3	Climb Check Cruise	No Change		1		1	1			
4	Climb Check Cruise		1		1	1		1		
5	Climb Check Cruise			1		1			1	
6	Climb Check Cruise	No Change			1	1				1
7	Climb Check Cruise		1			1	1			
8	Climb Check Cruise		1		1	1				
9	Climb Check Cruise	No Change	1			1	1			
10	Climb Check Cruise		1		1	1		1		

TABLE IV (Continued)
 FATIGUE SPECTRUM -ADDITIONAL LOADS

BLOCK	ITEM	θ								
		.35	.45	.55	.65	.75	.85	.95	1.05	1.15
11	Climb Check Cruise	No Change	1 1	1		1				
12	Climb Check Cruise		1	1	1	1		1		
13	Climb Check Cruise	No Change	1				1			
14	Climb Check Cruise		1	1	1	1	1			
15	Climb Check Cruise	No Change	1 1	1 1			1			1
16	Climb Check Cruise		1 1		1			1		
17	Climb Check Cruise	No Change	1 1							
18	Climb Check Cruise		1		1	1	1			
19	Climb Check Cruise		1 1	1		1 1				
20	Climb Check Cruise		1	1	1	1				

TABLE IV (Continued)

FATIGUE SPECTRUM-ADDITIONAL LOADS

BLOCK	ITEM	θ								
		.35	.45	.55	.65	.75	.85	.95	1.05	1.15
21	Climb Check Cruise	No	1 Change 1			1				
22	Climb Check Cruise		1		1	1				
23	Climb Check Cruise	No	1 Change 1			1				
24	Climb Check Cruise		1		1	1	1			
25	Climb Check Cruise	No	1 Change 1			1				
26	Climb Check Cruise		1	1	1	1	1			
27	Climb Check Cruise	No	1 Change 1	1		1		1		
28	Climb Check Cruise		1	1	1		1			
29	Climb Check Cruise		1			1	1			
30	Climb Check Cruise		1		1	1		1		

TABLE IV (Continued)

FATIGUE SPECTRUM-ADDITIONAL LOADS

BLOCK	ITEM	θ								
		.35	.45	.55	.65	.75	.85	.95	1.05	1.15
31	Climb Check Cruise	No Change	1 Change 1	1		1				
32	Climb Check Cruise		1 1	1	1	1	1			
33	Climb Check Cruise	No Change		1		1	1			
34	Climb Check Cruise	1	1		1	1		1		
35	Climb Check Cruise	No Change	1	1		1	1			
36	Climb Check Cruise		1		1	1				
37	Climb Check Cruise	No Change	1	1						1
38	Climb Check Cruise		1 1	1	1	1	1			
39	Climb Check Cruise	No Change 1	1			1			1	
40	Climb Check Cruise		1		1	1	1			

TABLE IV (Concluded)
FATIGUE SPECTRUM-ADDITIONAL LOADS

BLOCK	θ ITEM	.35	.45	.55	.65	.75	.85	.95	1.05	1.15
		41	Climb Check Cruise	No Change	1 No Change	1		1		1
42	Climb Check Cruise		1		1	1		1		
43	Climb Check Cruise	No Change No Change		1		1	1			
44	Climb Check Cruise		1		1	1				
45	Climb Check Cruise		1	1		1				
46	Climb Check Cruise		1		1	1				
47	Climb Check Cruise	No Change		1		1				
48	Climb Check Cruise		1		1	1				
49	Climb Check Cruise	No Change	1			1				
50	Climb Check Cruise		1	1	1	1			1	

NOTES FOR TABLES II, III and IV

NOTES:

1. W^* = instantaneous gross weight/take-off gross weight
= 1.0 for take-off and climb
= 0.70 for check flights
= 0.75 for cruise
2. Operational GAG cycle: -12,500 psi to +25,000 psi
3. Check flight GAG cycle: -12,500 psi to +17,500 psi
4. Cruise loads shown in order of application.
5. Mean stress for cruise loads must have thermal stress component added. $S_{\text{mean}} = (S_{1g_D})(W^* + 0.65)$
6. Upon completion of first block of tests, Table IV must be used to determine necessary modifications to subsequent blocks.

TABLE V

STRAIN GAGE READINGS FROM
R.T. PROOF LOADING
SPECIMEN NO. 1

Gage No. and Location	Actuator Load				
	5 000 lb	10 000 lb	15 000 lb	17 500 lb	20 000 lb
	ϵ , in/in S, psi	ϵ , in/in S, psi	ϵ , in/in S, psi	ϵ , in/in S, psi	ϵ , in/in S, psi
7 (1) Stringer	.00026 5 120	.00052 10 240	.00079 15 600	.00092 18 100	.00106 20 900
8 Stringer	.00029 5 710	.00060 11 820	.00090 17 750	.00105 20 700	.00122 24 100
9 Stringer	.00027 5 320	.00055 11 850	.00083 16 350	.00098 19 300	.00113 22 300
10 Stringer	.00029 5 710	.00058 11 430	.00085 16 750	.00099 19 500	.00114 22 500
11 ^a Stringer	.00025 4 920	.00050 9 840	.00075 14 800	.00087 17 150	.00100 19 700
16 Splice Plate	.00033 6 500	.00065 12 800	.00100 19 700	.00115 22 650	.00130 25 600
17 Splice Plate	.00033 6 500	.00066 13 000	.00100 19 700	.00116 22 850	.00134 26 400
21 Door Dblr	.00042 8 270	.00075 14 800	.00125 24 600	.00142 27 950	.00160 31 500

TABLE V (Concluded)

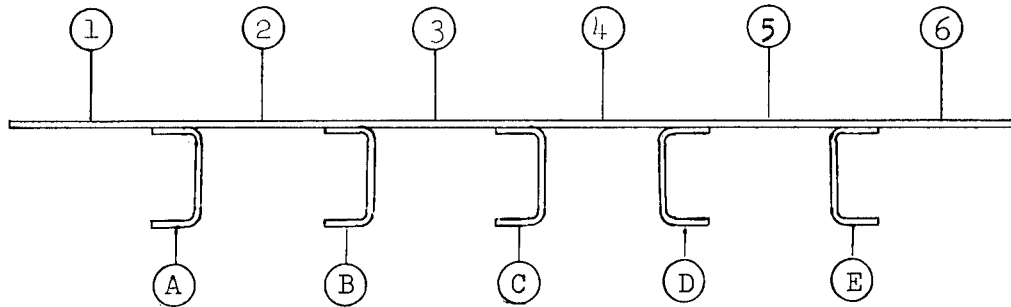
STRAIN GAGE READING FROM
550°F PROOF LOADING
SPECIMEN NO. 1

Gage No. and Location	Actuator Load			
	4 000 lb	8 000 lb	12 000 lb	16 000 lb
	ϵ in/in S, psi	ϵ in/in S, psi	ϵ in/in S, psi	ϵ in/in S, psi
7 Stringer	.000230 4 120	.000445 7 960	.000670 11 990	.000895 16 020
8 Stringer	.000253 4 530	.000507 9 080	.000762 13 630	.000900 16 110
9 Stringer	.000250 4 480	.000505 9 040	.000743 13 300	.000990 17 720
10 Stringer	.000265 4 740	.000489 8 750	.000715 12 800	.000980 17 540
11 Stringer	.000215 3 850	.000418 7 480	.000632 11 310	.000843 15 100
16 Splice Plate	.000263 4 710	.000553 9 900	.000867 15 520	.001178 21 050
17 Splice Plate	.000247 4 420	.000545 9 760	.000835 14 950	.001120 20 030
A (2) Test Skin	.000260 4 650	.000516 9 240	.000765 13 690	.001019 18 240
B (2) Test Skin	.000231 4 140	.000462 8 270	.000695 12 430	.000935 16 730
C (2) Test Skin	.000306 5 480	.000644 11 520	.000968 17 320	.001298 23 220
D (2) Test Skin	.000265 4 740	.000570 10 200	.000965 15 490	.001170 20 950
E (2) Test Skin	.000350 6 260	.000710 12 710	.001065 19 080	.001415 25 340
H (2) Test Skin	.000320 5 730	.000645 11 530	.000982 17 570	.001295 23 190

NOTES:

1. See figure 14 for strain gage locations.
2. Strain gages on outer surface of skin panel.
3. ϵ = strain in inches/inch; S = stress in psi

TABLE VI
RESULTS OF THICKNESS SURVEY CONDUCTED
ON TEST SPECIMENS



Location		1	2	3	4	5	6	A	B	C	D	E
Spec No.												
1	Max	.045	.046	.046	.042	.046	.046	.046	.045	.046	.043	.044
	Min	.041	.041	.041	.041	.042	.042	.040	.041	.041	.041	.039
2	Max	.048	.049	.048	.048	.048	.048	.047	.046	.046	.050	.044
	Min	.041	.041	.041	.040	.040	.039	.041	.041	.041	.044	.042
3	Max	.045	.045	.045	.046	.047	.046	.044	.044	.044	.047	.045
	Min	.042	.042	.042	.042	.040	.041	.039	.043	.038	.047	.044
4	Max	.046	.044	.044	.044	.044	.044	.048	.050	.046	.049	.046
	Min	.041	.040	.041	.041	.041	.042	.045	.041	.041	.043	.043
5	Max	.048	.048	.048	.047	.046	.046	.044	.049	.046	.045	.045
	Min	.040	.046	.046	.046	.044	.044	.042	.041	.045	.042	.041
6	Max	.046	.046	.046	.047	.047	.046	.041	.049	.048	.048	.046
	Min	.044	.045	.045	.044	.044	.046	.041	.041	.039	.046	.042
7	Max	.049	.049	.049	.049	.047	.047	.048	.048	.048	.043	.046
	Min	.039	.039	.039	.039	.039	.039	.047	.042	.041	.039	.043
8	Max	.044	.043	.043	.045	.045	.045	.043	.045	.046	.050	.046
	Min	.042	.041	.042	.042	.041	.041	.041	.042	.042	.047	.043

NOTES:

The maximum and minimum values shown were observed over the 48 inch test section only - measurements were not taken in other areas.

TABLE VII
INSPECTION LOG-SPECIMEN NUMBER 2

Crack Number	Cycles				
	31 344	31 845	32 345	32 845	33 345
1	1.37	1.44	1.53	1.56	1.60
2	.46	.53	.70	.79	.82
3	.90	.95	1.06	1.17	1.19
4	.80	.84	.86	.90	.91
5	1.05	1.09	1.15	1.18	1.19
6		.03	.03	.03	.03
7	.13	.13	.13	.13	.13
8	.16	.16	.16	.16	.16
9	.40	.40	.42	.43	.44
10	.47	.48	.50	.51	.53
11	.52	.55	.57	.58	.59
12	.40	.42	.43	.45	.47
13	.33	.35	.37	.37	.38
14	.51	.54	.54	.54	.54
15	.31	.34	.35	.36	.37
16	.41	.44	.45	.48	.51
17	.22	.22	.22	.22	.22
18	.68	.68	.70	.71	.73
19	.54	.54	.56	.58	.59
20	.46	.50	.50	.52	.55
21	.38	.38	.39	.43	.45
22	.39	.39	.40	.42	.44
23	.49	.54	.54	.54	.55
24	.26	.31	.31	.33	.34
25	.33	.33	.34	.34	.34

TABLE VII (Concluded)
INSPECTION LOG-SPECIMEN NUMBER 2

Crack Number	Cycles				
	31 344	31 845	32 345	32 845	33 345
26	0.18	0.21	0.21	0.21	0.21
27	.43	.43	.43	.44	.45
28	.35	.40	.40	.40	.40
29	.20	.22	.24	.24	.25
30	.10	.20	.20	.20	.20
31	.44	.48	.50	.50	.51
32	.25	.33	.34	.35	.35
33	.90	.92	.95	.96	.97
34	.67	.70	.72	.72	.72
35	.96	1.00	1.04	1.04	1.05
36	.96	.99	1.04	1.07	1.10
37	.25	.26	.26	.27	.28
38	.47	.47	.47	.48	.62
39		.07	.08	.08	.08
40		.06	.07	.07	.07
41			.24	.28	.28

NOTES:

1. Beam tested under G.A.G. loads, $S_{max} = 25$ ksi, $S_{min} = 12.5$ ksi
2. Fatigue cracks not detected until 31 344 cycles.
3. See Figure 16 for crack locations.

TABLE VIII

INSPECTION LOG-SPECIMEN NUMBER 3

Crack Number	Cycles				
	59 846	74 106	88 048	100 515	106 717
1	0.23	0.41	0.60	0.68	0.80
2		.06	.10	.11	.12
3		.34	.49	.67	.79
4		.04	.06	.10	.10
5		.08	.16	.26	.32
6			.24	.34	.40
7					.10
8					.10

Crack Number	Cycles				
	118 500	127 242	140 901	156 032	159 955
1	0.94	1.10	1.32	1.72(2)	1.87(2)
2	.13	.13	.14	.16	.20
3	.94	1.12	1.37(2)	1.57(2)	1.59(3)
4	.12	.17	.20	.22	.23
5	.46	.58	.78	1.03	1.24
6	.49	.59	.77	.99	1.19(2)
7	.21	.25	.35	.47	.55
8	.18	.23	.36	.50	.52
9				.18	.36(2)
10				.12	.19
11				.09	.26
12				.10	.11
13					(3)
14					(3)

NOTES:

1. Test conducted at 550°F, $S_{max} = 41.25$ ksi, $S_{min} = 28.75$ ksi
2. Visible strain deformation
3. Crack joins adjacent crack or hole.
4. See Figure 17 for crack locations.

TABLE IX
INSPECTION LOG-SPECIMEN NUMBER 4

Crack Number	Flights						
	750	1250	1500	1750	2000	2250	2500
1	(2)	0.54	0.54	0.54	0.62	0.66	1.05
2	(2)	.32	.32	.32	.38	.42	.92
3	(2)	.38	.42	.42	.47	.40	.42(3)
4	(2)	.56	.58	.58	.63	.70	.56(3)
5	(2)	.64	.64	.64	.70	.75	.71(4)
6	(2)	.50	.52	.54	.58	.70	.57(4)
7	(2)	.40	.43	.43	.43	.56	.51(5)
8	(2)	.58	.65	.65	.65	.68	.53(5)
9	(2)	.28	.28	.28	.36	.36	.62(6)
10	(2)	.22	.30	.30	.35	.35	(6)
11	(2)	.16	.18	.18	.22	.22	(6)
12	(2)	(2)	(2)	.18	.22	.26	(6)
13	(2)	(2)	(2)	.22	.24	.26	.50(6)
14	(2)	(2)	(2)	.12	.20	.20	.23
15	(2)	(2)	.22	.22	.28	.31	(7)
16	(2)	(2)	(2)	(2)	(2)	.14	.50
17	(2)	(2)	.18	.18	.20	.22	.50
18	(2)	(2)	.27	.27	.30	.30	.62
19	(2)	(2)	(2)	(2)	.15	.15	.35
20		.08	.12	.12	.13	.15	(4)
21		(2)	(2)	(2)	(2)	.18	(6)
22		(2)	(2)	(2)	.12	.18	.20(7)
23		.24	.24	.24	.28	.28	(7)
24		(2)	(2)	(2)	(2)	(2)	.58
25		(2)	(2)	.10	.12	.14	.53
26		.26	.28	.28	.30	.30	.58
27		(2)	.17	.17	.22	.23	.42
28		.22	.22	.22	.22	.22	.46
29		(2)	.18	.20	.24	.25	.52
30		(2)	(2)	(2)	.06	.08	.08
31		(2)	(2)	(2)	(2)	(2)	.43(7)
32		(2)	(2)	(2)	(2)	.10	.52
33		(2)	(2)	(2)	(2)	.11	.33
34		(2)	(2)	.08	.09	.14	.37

TABLE IX (Continued)
INSPECTION LOG-SPECIMEN NUMBER 4

Crack Number	Flights						
	750	1250	1500	1750	2000	2250	2500
35		(2)	0.20	0.23	0.26	0.26	0.51
36		(2)	0.16	0.16	.17	.17	.40
37		(2)	(2)	(2)	.16	.16	.34
38		(2)	(2)	(2)	(2)	(2)	.32
39		(2)	(2)	(2)	(2)	.08	.29
40		(2)	(2)	.15	.17	.18	.45
41		(2)	(2)	(2)	(2)	(2)	.22
42		(2)	(2)	.07	.12	.14	.37
43		(2)	(2)	(2)	(2)	(2)	.31
44		(2)	(2)	(2)	(2)	(2)	.45
45			(2)	(2)	(2)	(2)	.36
46				(2)	(2)	(2)	.20
47							.40
48							.30
49							.33
50							.13
51							.28
52							.12
53							.21
54							(3)
55							.56
56							.81
57							.48
58							(6)
59							.27
60							.27
61							.30
62							(2)
63							.20
64							(2)
65							(5)

TABLE IX (Concluded)
INSPECTION LOG-SPECIMEN NUMBER 4

NOTES:

1. Tested under spectrum loading, $S_{1_{\text{GD}}} = 25$ ksi
2. Visible strain deformation.
3. Joined thru rivet at location 54, total $l = 2.87$
4. Joined thru rivet at location 20, total $l = 2.91$
5. Joined thru rivet at location 65, total $l = 2.82$
6. Crack 9 joined 13 thru intermediate cracks, total $l = 6.04$
7. Joined thru locations 15 and 23, total $l = 3.11$

TABLE X
INSPECTION LOG-SPECIMEN NUMBER 5

		Cycles					
Crack Number	9 673	17 411	18 106	20 000	22 500	23 044	26 014
1	0.07	0.22	0.23	0.25	0.30	0.46	0.63
2		(2)	(2)	(2)	(2)	(2)	(2)

		Cycles					
Crack Number	27 257	28 339	30 900	31 208	33 197	34 283	36 192
1	0.75	0.88	1.13	1.14	1.35(3)	1.38(3)	1.45(3)
2	(2)	(2)	(2)	(2)	(2)	(2)	(2)
3	.03	.07	.14	.15	.17	.18	.33
4		.03	.09	.10	.19	.23	.37
5					.18	.23	.43
6					.10	.11	.15
7						.03	.22

		Cycles					
Crack Number	37 197	39 495	41 495	42 753	44 395	46 295	48 301
1	1.45(3)	1.45(3)	1.45(3)	1.45(3)	1.45(3)	1.45(3)	1.45(3)
2	(2)	(2)	(2)	(2)	(2)	(2)	(2)
3	.40	.57	.85	.93	1.23	1.92	2.93
4	.45	.74	1.08(3)	1.13(3)	1.15(3)	1.20(3)	1.25(3)
5	.50	.70	1.00	1.10	1.37(3)	1.95(3)	2.75(3)
6	.19	.21	.28	.30	.36	.43	.45
7	.29	.50	.95	1.06	1.27	1.56	3.01
8	.20	.21	.24	.24	.27	.27	.27
9	.04	.05	.09	.09	.10	.10	.12
10		.26	.37	.38	.42	.52	.57
11		.39	.48	.50	.55	.62	.66
12		(2)	(2)	(2)	(2)	(2)	(2)
13			.16	.24(3)	.46(3)	.78(3)	2.72(3)
14				.06	.06	.07	.08

NOTES:

1. Tested under G.A.G. loading, $S_{max} = 25$ ksi, $S_{min} = -12.5$ ksi
2. Strain deformed area which did not expand or form cracks.
3. Crack meets adjacent hole or crack.

TABLE XI
INSPECTION LOG-SPECIMEN NUMBER 6

Crack Number	Flights						
	5 750	6 000	6 250	6 500	7 500	8 000	8 500
1	0.07	0.09	0.12	0.18	0.22	0.22	0.23
2	.03	.06	.07	.17	.22	.22	.24
3				.11	.23	.24	.26
4				.41	.57	.57	.60
5					(2)	.05	.07

Crack Number	Flights						
	9 000	9 500	10 000	11 000	11 500	12 000	12 500
1	0.29	0.39	0.52	0.75	0.84	0.96	1.05
2	.32	.33	.40	.51	.60	.64	.67
3	.35	.40	.46	.72	1.02(3)	1.17(3)	1.18(3)
4	.64	.76	.80	1.05	1.18(3)	1.28(3)	1.36(3)
5	.08	.09	.10	.12	.12	.12	.15
6	.03	.10	.14	.17	.20	.27	.35(4)
7	.04	.04	.06	.07	.13	.18	.22
8	.07	.13	.21	.29	.35	.43	.50
9	.13	.29	.32	.50	.56	.59	.62
10	(2)	(2)	.02	.11	.15	.20	.25(4)
11				.15	.30	.42	.58
12				.05	.05	.06	.07
13					(3)	(3)1=3.27	(3)1=3.38
14						.03	.16
15						.03	.04
16						.32	.42
17						.03	.03

NOTES:

1. Tested under spectrum loading, $S_{1/2D} = 25$ ksi.
2. Visible strain deformation.
3. Cracks 3 and 4 joined thru crack 13.
4. Cracks 6 and 10 joined.

TABLE XII
INSPECTION LOG-SPECIMEN NUMBER 7

Crack Number	Cycles						
	48 273	60 367	73 723	87 465	101 579	112 670	122 115
1	0.06	0.13	0.23	0.37	0.53	0.67	0.81
2		.06	.14	.23	.37	.49	.65
3					.25	.43	.62
4					.03	.05	.07
5					.03	.05	.07
6					.03	.19	.27
7					.07	.25	.35
8					.02	.19	.24
9					.04	.12	.15
10					.08	.13	.18
11					.13	.23	.27
12					.13	.21	.25
13					.03	.06	.16
14					.06	.10	.13
15					.19	.29	.34
16					.02	.06	.10
17					.05	.17	.21
18					.14	.19	.23
19					.02	.02	.02
20					.50	.66	.80
21						.02	.04
22						.07	.09
23						.10	.12
24							.05
25							.07
26							.15

TABLE XII (Concluded)

INSPECTION LOG-SPECIMEN NUMBER 7

Crack Number	Cycles			Crack Number	Cycles		
	129 141	140 278	154 047		129 141	140 278	154 047
1	1.00	1.34(2)	1.56(2)	25	.10	.11	.13
2	.78	1.09	1.30	26	.20	.21	.31
3	.63	.71	.85	27	.04	.29(2)	.36(2)
4	.07	.07	.07	28	.02	.05	.09
5	.08	.11	.14	29	.41	.54	.65
6	.33	.42	.55	30	.05	.09	.12
7	.40	.72(3)	.93(3)	31	.05	.08	.13
8	.28	1.00(3)	1.00(3)	32	.07	.14	.19
9	.20	.62	.82	33	.08	.12	.14
10	.25	.66(4)	.84(4)	34	.03	.06	.06
11	.32	1.00(4)	1.00(4)	35	.11	.15	.26
12	.35	.75	.92(4)	36	0.06	0.09	0.10
13	.19	.26	.69(5)	37	.01	.01	.08
14	.17	.25	.58(5)	38	.09	.03	.16
15	.41	.51	.73(6)	39		.15	.19
16	.12	.12	.52(6)	40		.05	.09
17	.33	.33	.44	41			.10
18	.35	.35	.44	42			.04
19	.03	.05	.13	43			.04
20	.86	1.01	1.21	44			.03
21	.05	.05	.07	45			.11
22	.09	.09	.13	46			.10
23	.19	.23	.33	47			.08
24	.08	.10	.16				

NOTES:

1. Test conducted at 550°F, $S_{max} = 41.25$ ksi, $S_{min} = 28.75$ ksi
2. Cracks 1 and 2 joined thru position 27.
3. Cracks 7 and 9 joined thru position 8.
4. Cracks 10 and 12 joined thru position 11.
5. Cracks 13 and 14 joined.
6. Cracks 15 and 16 joined.

TABLE XIII
INSPECTION LOG-SPECIMEN NUMBER 8

Flights							
Crack Number	9 250	9 500	9 750	10 000	10 250	10 500	10 750
1	0.01	0.03	0.06	0.08	0.08	0.08	0.09
2	.01	.02	.03	.04	.04	.05	.05
3						.02	.02

Flights							
Crack Number	11 00	11 250	11 500	11 750	12 000	12 250	12 500
1	0.09	0.09	0.09	0.09	0.09	0.09	0.09
2	.05	.05	.06	.10	.10	.11	.11
3	.02	.03	.03	.03	.04	.04	.04

NOTES:

1. Tested under spectrum loading, $S_{1gD} = 25$ ksi.

TABLE XIV

COMPARISON OF PREDICTED AND EXPERIMENTAL
BOX BEAM LIVES UNDER SPECTRUM LOADS

(Failure assumed when $lc=.50$ in.)

Spec. No.	Constant Amplitude Loading				Spectrum Loading				
	Temp. $^{\circ}$ F	Est. Life Cycles (1)	Box Beam Life Cycles	Test Life Est. Life	Spec. No.	Est. Life Flights (2)	Predicted Life Flights (3)	Test Life Flights	Pred. Life Test Life
2	80	13 000	25 000	1.92	4	3100	5950	1 000	5.95
3	550	75 000	80 750	1.08	4	3100	3340	1 000	3.34
5	80	36 000	24 000	.67	6	7400	4950	6 815	.72
7	550	90 000	99 000	1.10	6	7400	8140	6 815	1.19
5	80	36 000	24 000	.67	8	7400	4950	>12 500	<.39
7	550	90 000	99 000	1.10	8	7400	8140	>12 500	<.65

NOTES:

1. Constant amplitude life of simple specimens per reference (2) and Appendix A.
2. Spectrum life computed according to linear cumulative damage theory and data contained in reference (2) and Appendix A.
3. Box beam predicted life:

$$\text{life} = (\text{computed spectrum life}) \times \frac{\text{Constant amplitude box beam life}}{\text{Simple spec. constant amplitude life}}$$

TABLE XV

RESULTS OF FATIGUE TESTS ON
LOAD CARRYING SPOTWELDS

Spec. Type (1)	Temp. °F	S _{max} ksi	S _{mean} ksi	Cycles to Failure (2)	Mean Cycles
2	RT	25	6.25	15 000	12 800
2	RT	25	6.25	11 000	
2	RT	25	6.25	10 000	
2	RT	25	6.25	14 000	
2	RT	25	6.25	15 000	
3	RT	80	25	5 000	1 920
3	RT	80	25	949	
3	RT	80	25	1 503	
3	RT	40	25	47 000	49 000
3	RT	40	25	58 000	
3	RT	40	25	43 000	
3	RT	60	25	8 000	7 050
3	RT	60	25	7 240	
3	RT	60	25	6 060	
3	550	40	25	31 000	41 500
3	550	40	25	49 000	
3	550	40	25	47 000	
3	550	55	25	6 420	6 700
3	550	55	25	9 260	
3	550	55	25	5 160	
3	550	70	25	3 080	2 250
3	550	70	25	1 730	
3	550	70	25	2 160	

NOTES:

1. See Figure 29 for specimen configurations.
2. All specimens failed thru net section, in the row of spotwelds closest to the loading hole.

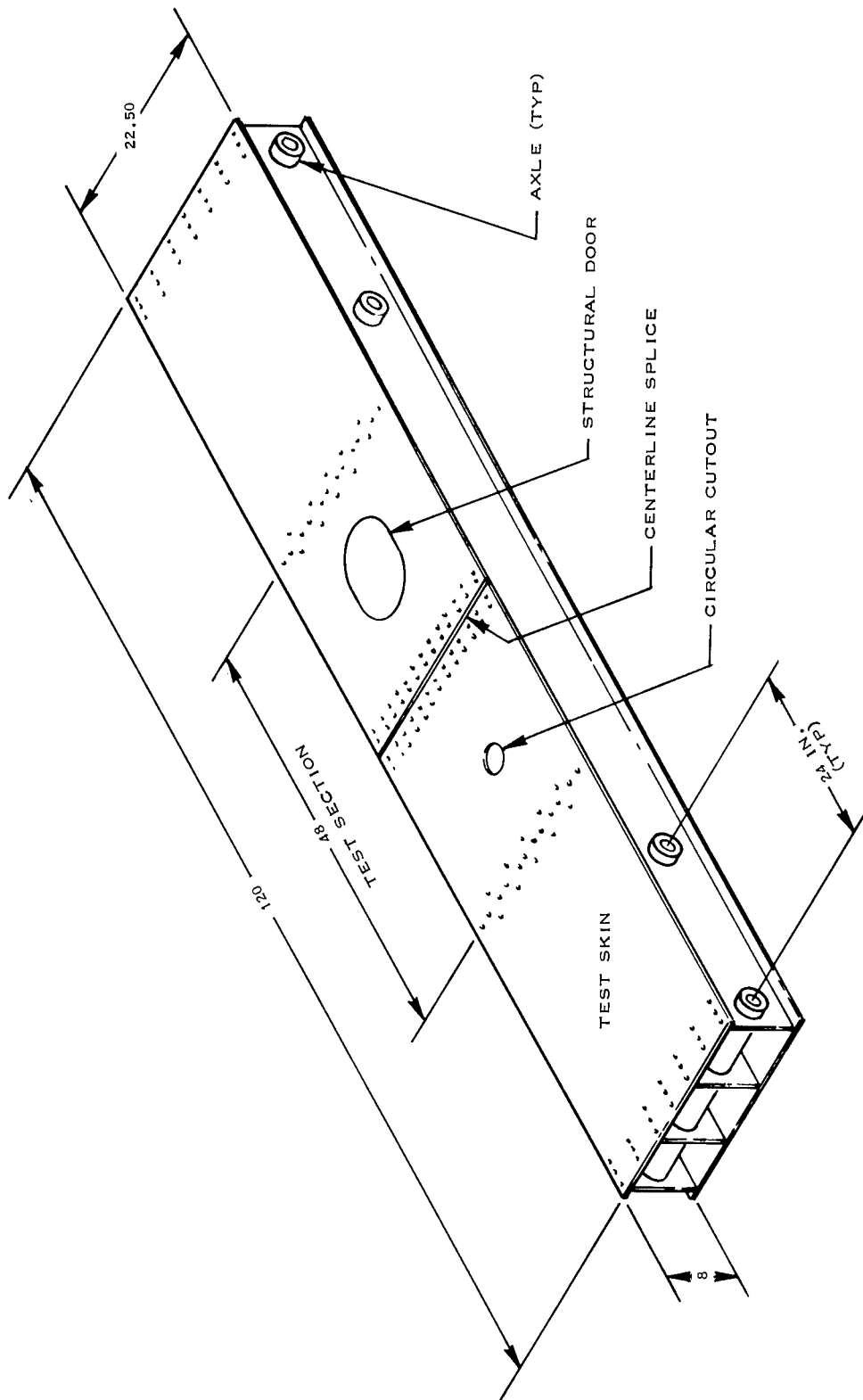


Figure 1. Sketch Showing General Arrangement of Box-Beam and Test Skin

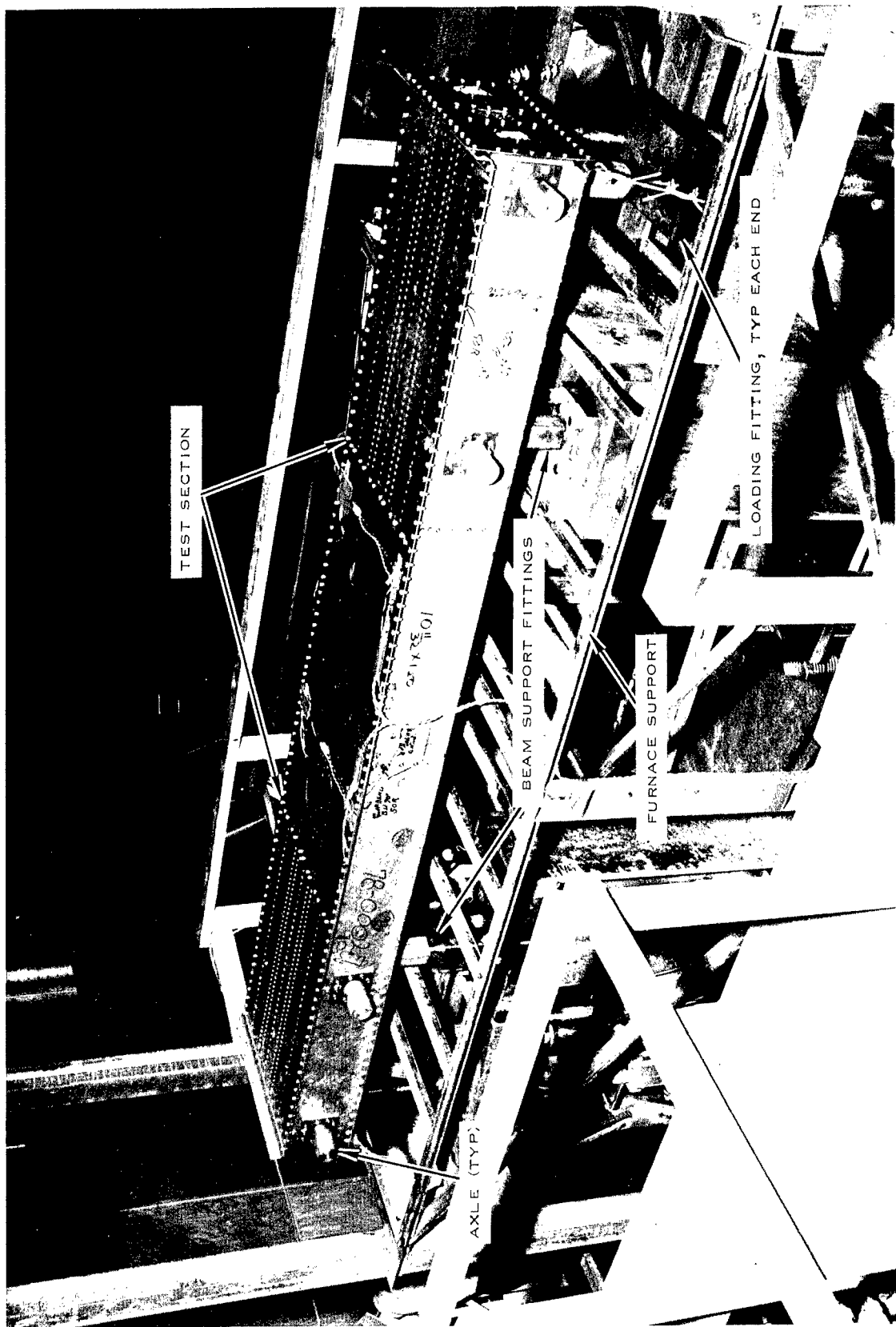


Figure 2. View Showing Complete Box Beam and Test Skin Installed in Test Fixture

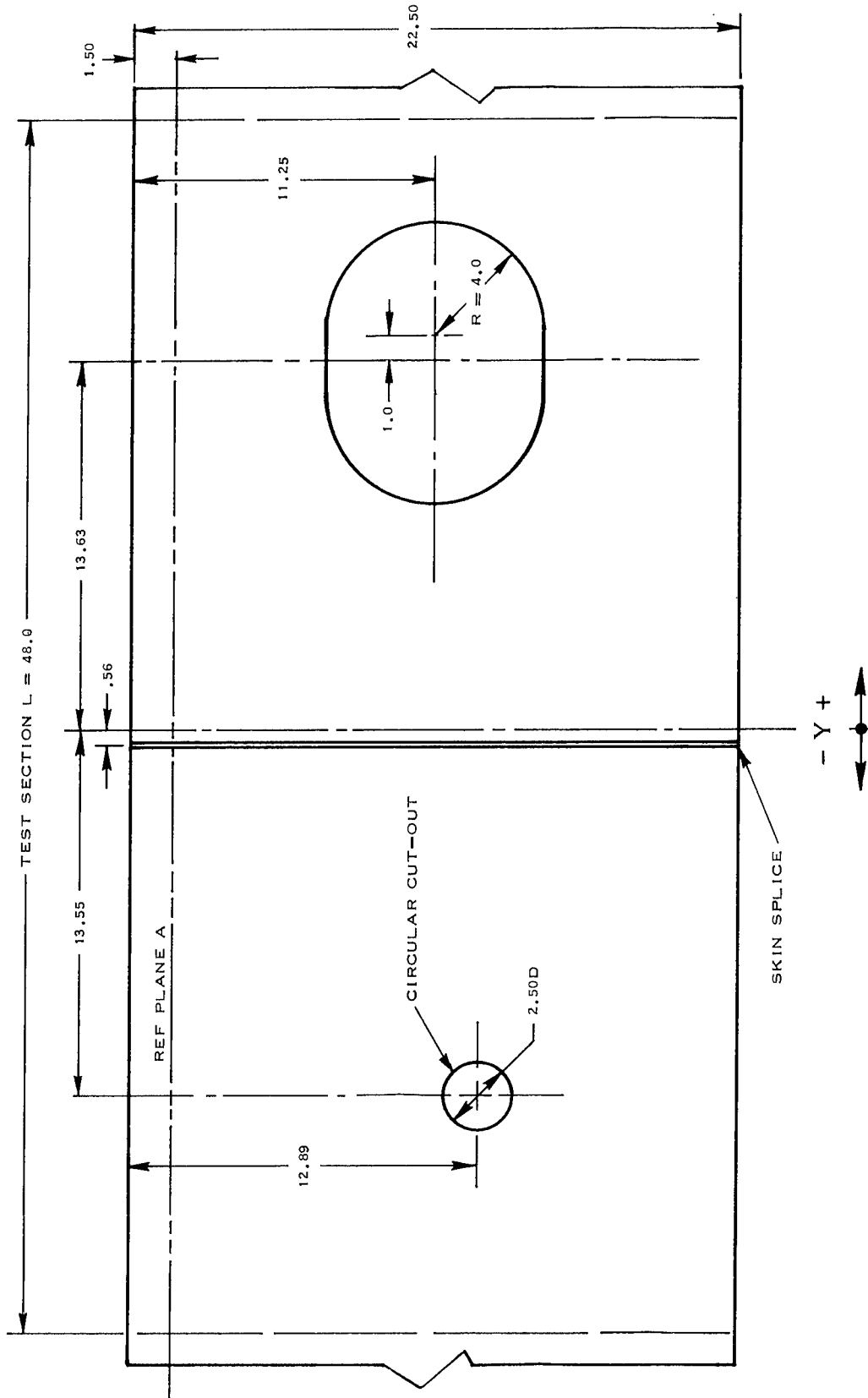


Figure 3. General Arrangement of Test Specimen

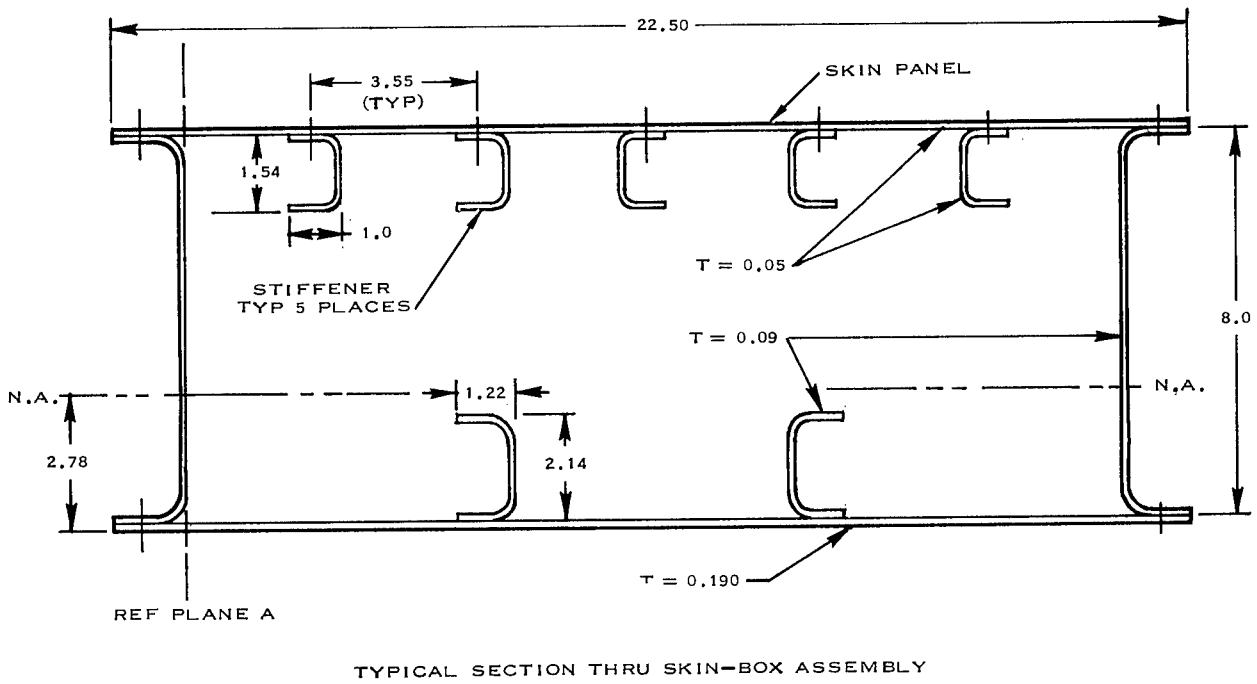
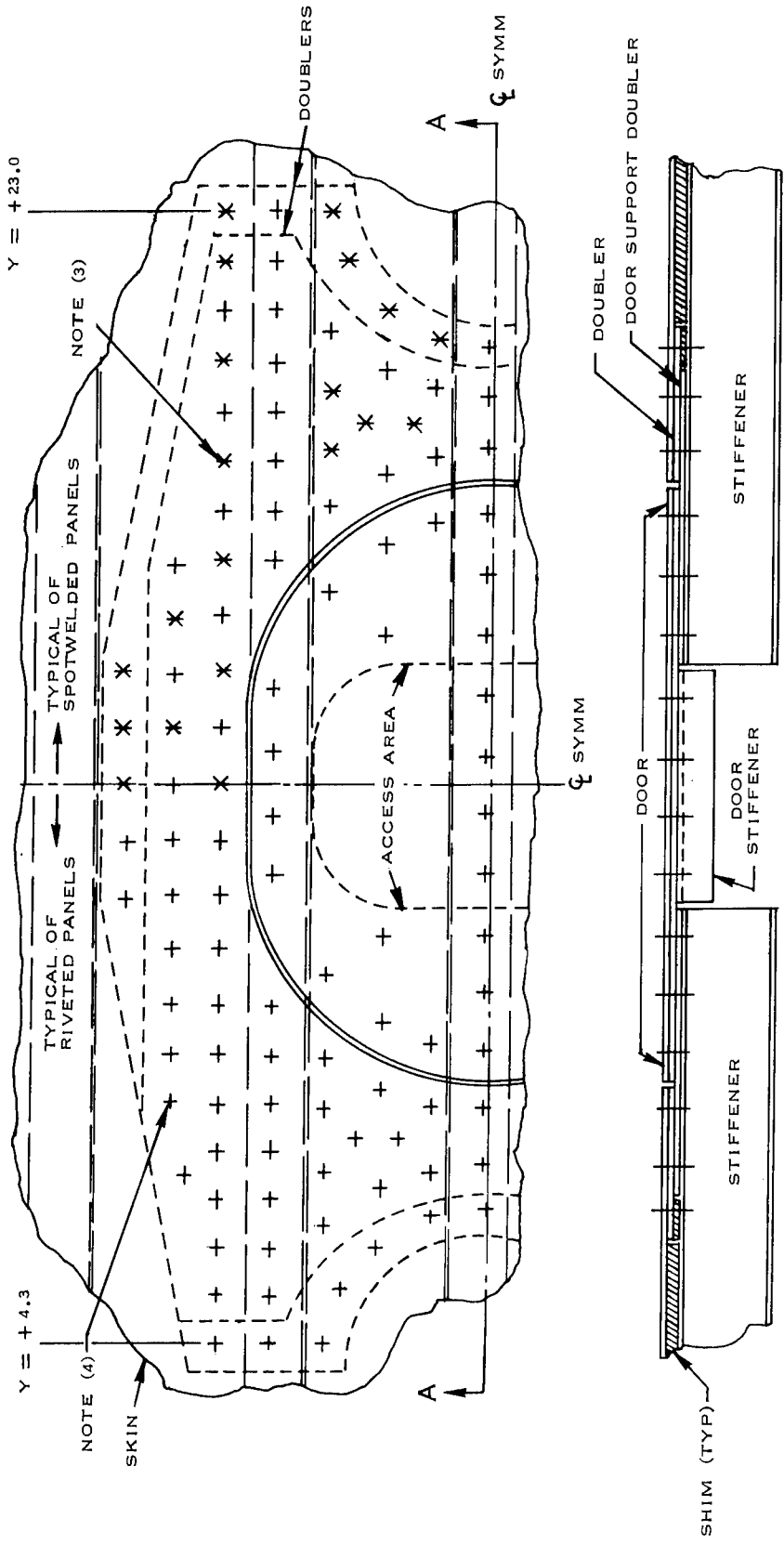


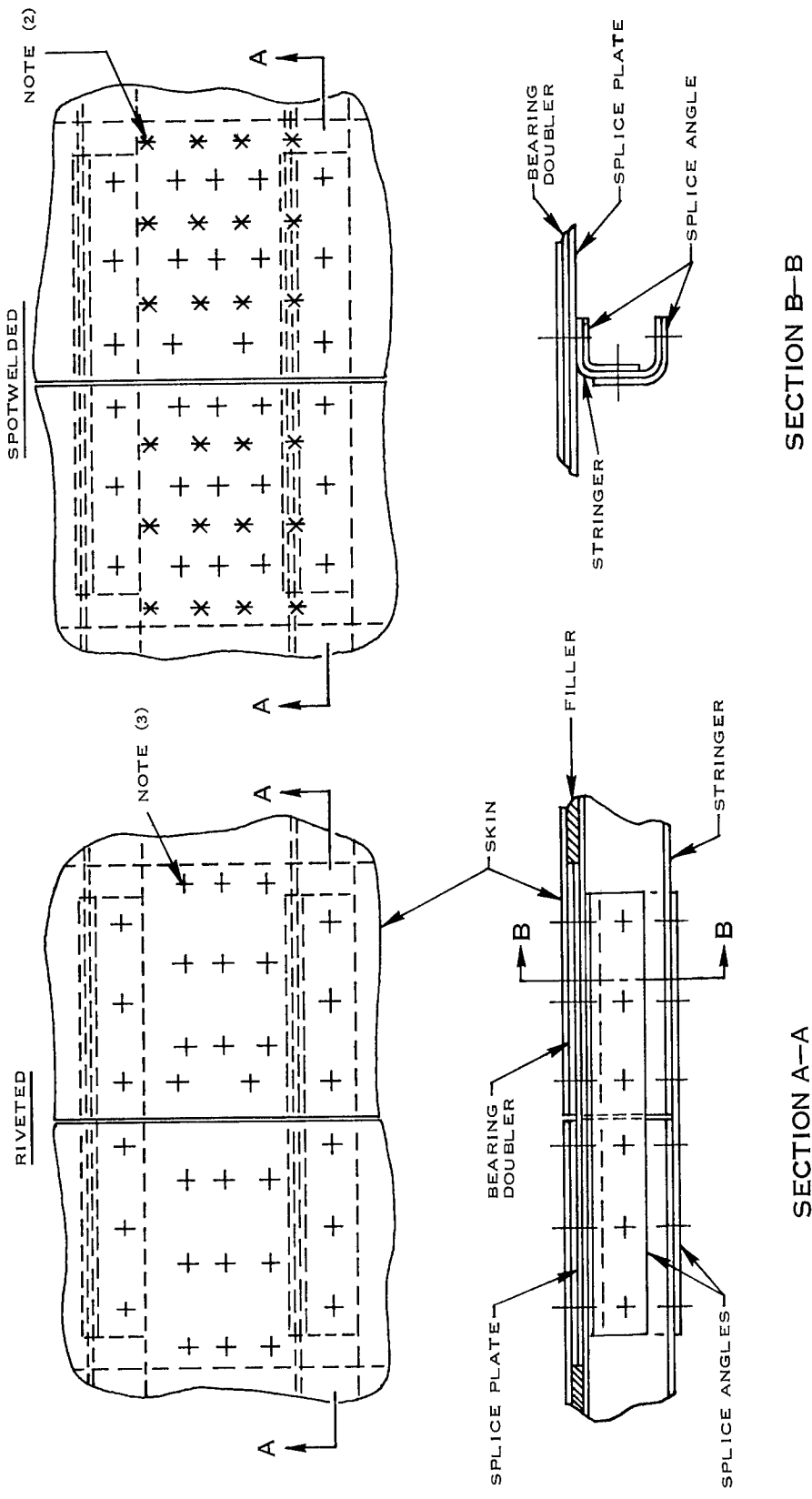
Figure 3. Concluded. General Arrangement of Test Specimen



SECTION A-A

- NOTES:
1. All stock, Ti-8AL-1Mo-1V, $t_{nom} = 0.050$
 2. Door and doublers symmetrical about 2 axes. Sketch shows S/W arrangement to right of Q, riveted to left
 3. Spotwelds * connect skin and door doubler only (Typical)
 4. Rivets + connect skin, both doublers and stiffeners

Figure 4. Sketch Showing Details of Structural Door



- NOTES:
1. All doublers and splice members $t_{nom} = 0.050$
 2. Spotwelds * connect skin and bearing doubler only
 3. Rivets + connect skin, bearing doubler and splice plate
 4. Sections A-A and B-B are common to both types of construction

Figure 5. Sketch Showing Details of Centerline Splice

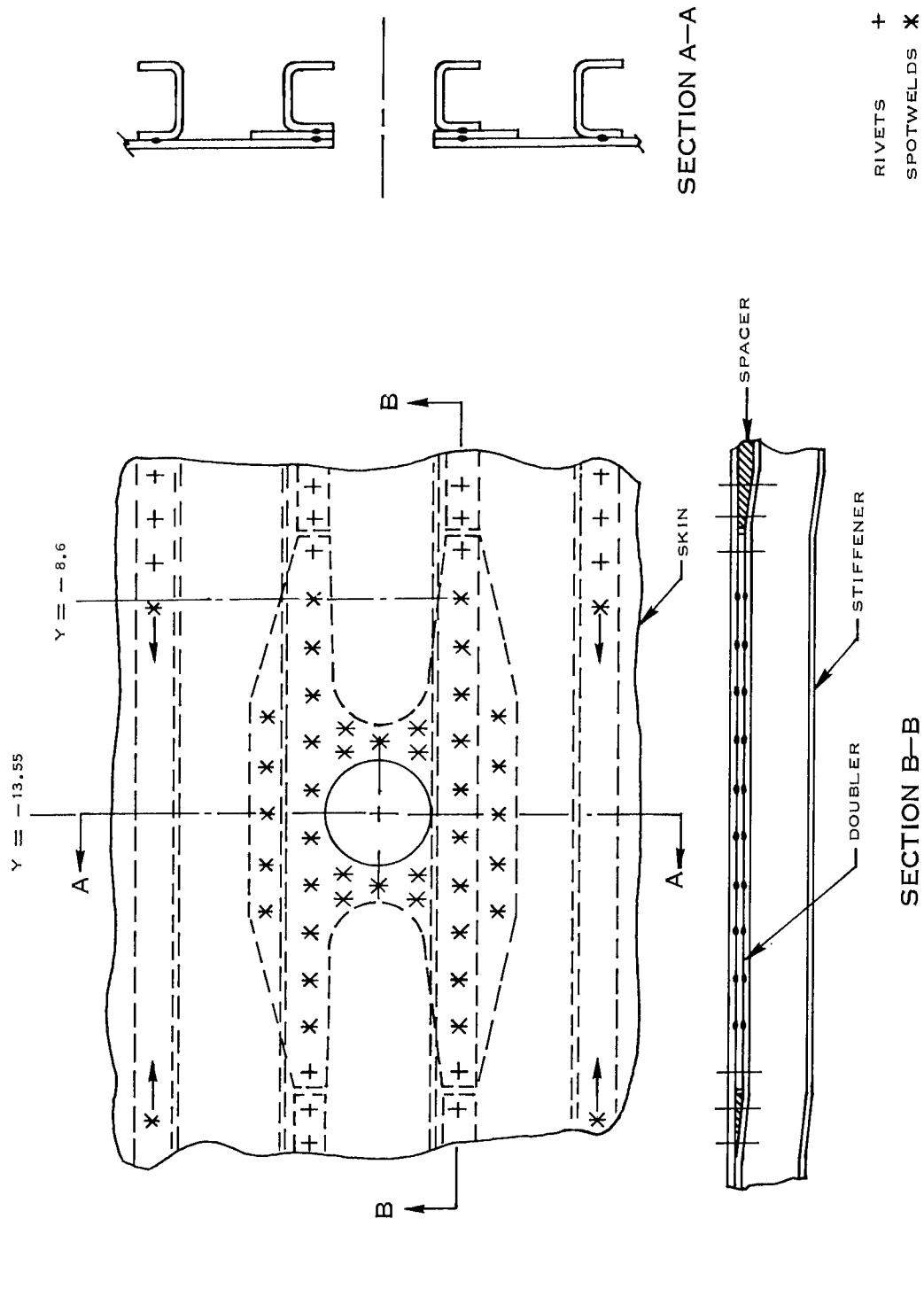


Figure 6. Sketch Showing Details of Circular Cut-out



Figure 7. Internal Arrangement of Basic Box

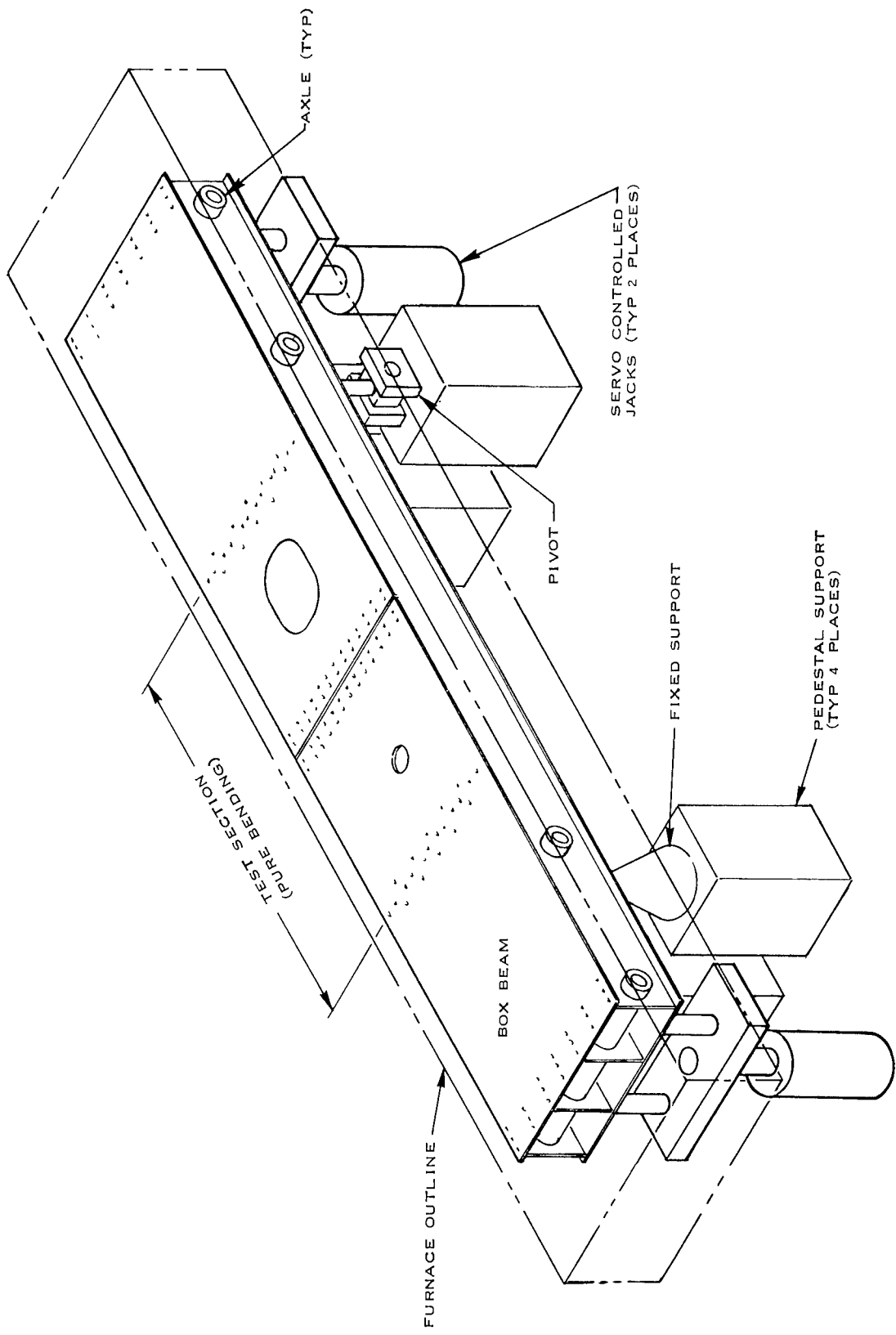


Figure 8. Sketch Showing Box Beam Loading Arrangement



Figure 9. View of Box Beam in Furnace. One Side of Furnace Removed for Clarity

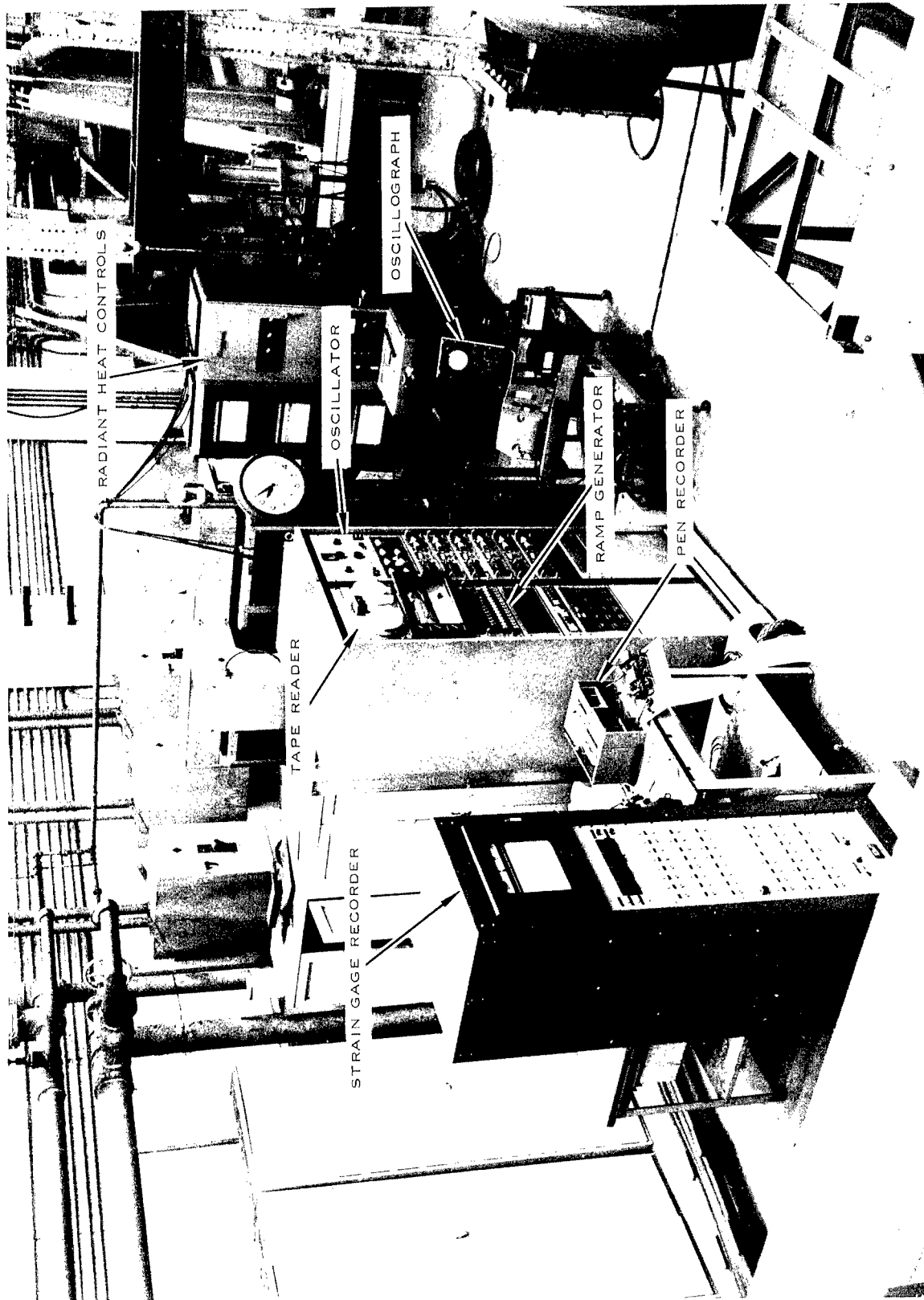


Figure 10. Overall View of Control Equipment

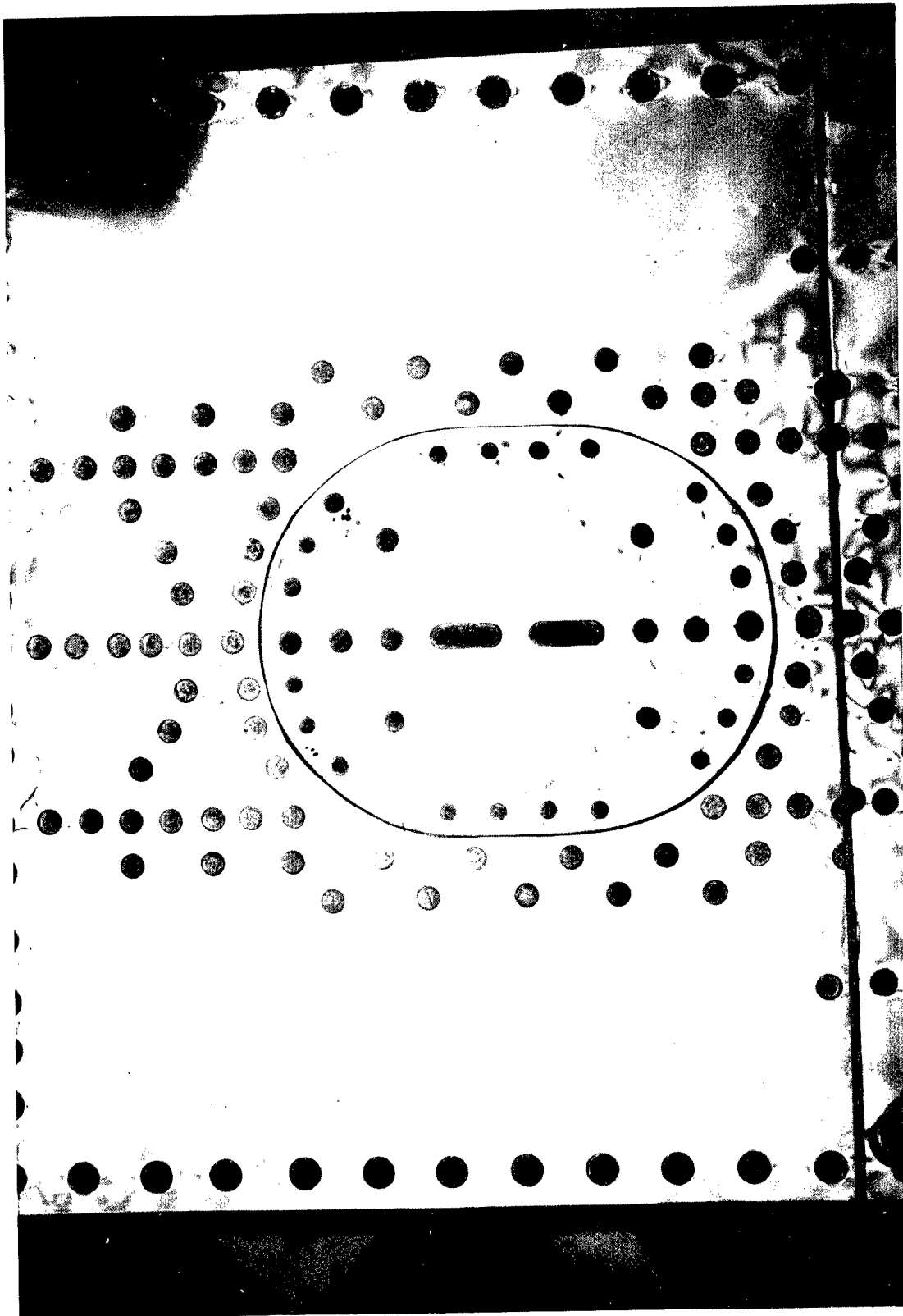


Figure 11. Photostress Evaluation, Box Beam Number 1.
View Showing Isochromatics Around Structural Door

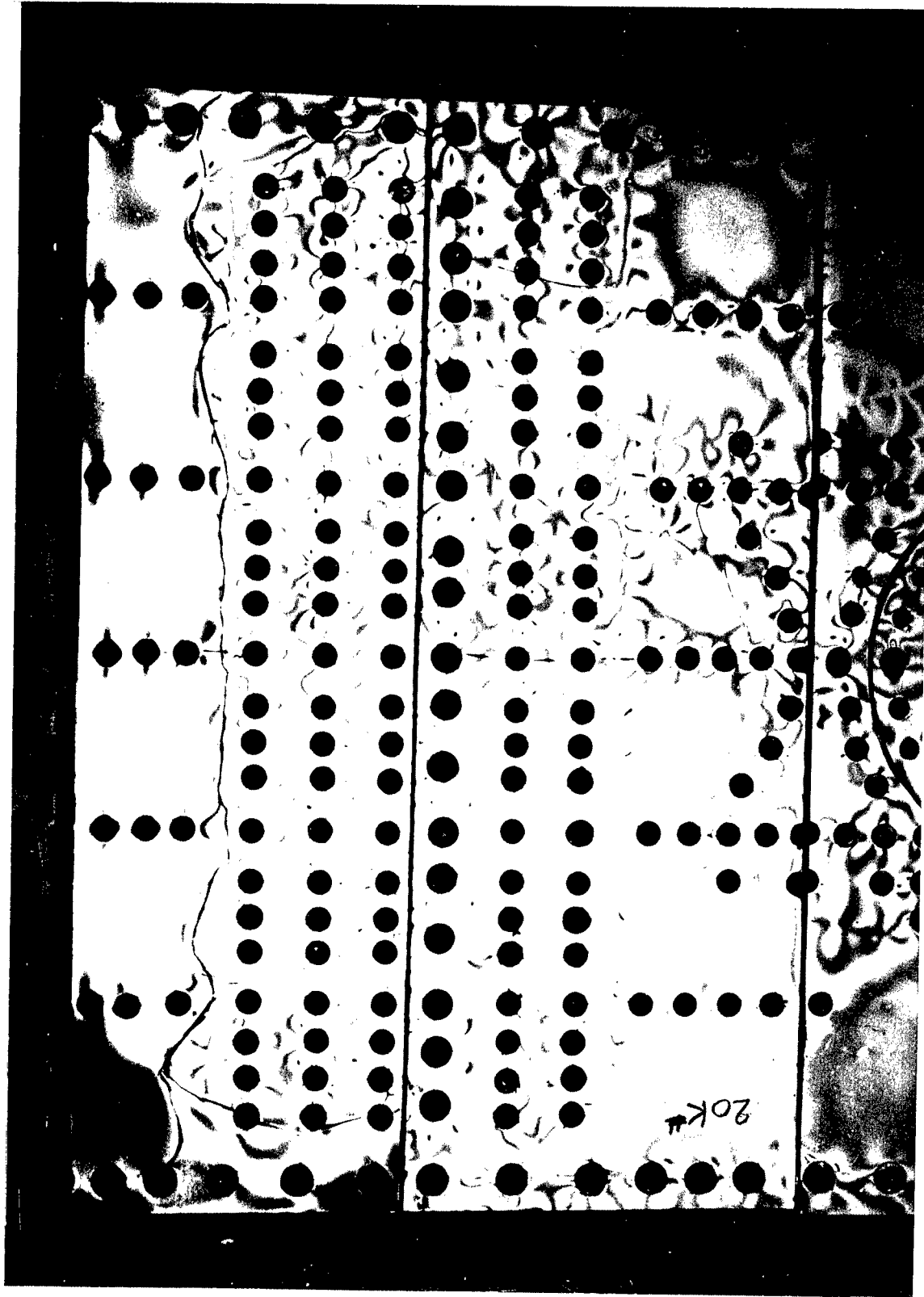


Figure 12. Photostress Evaluation, Box Beam Number 1.
View Showing Isochromatics Around Centerline Splice

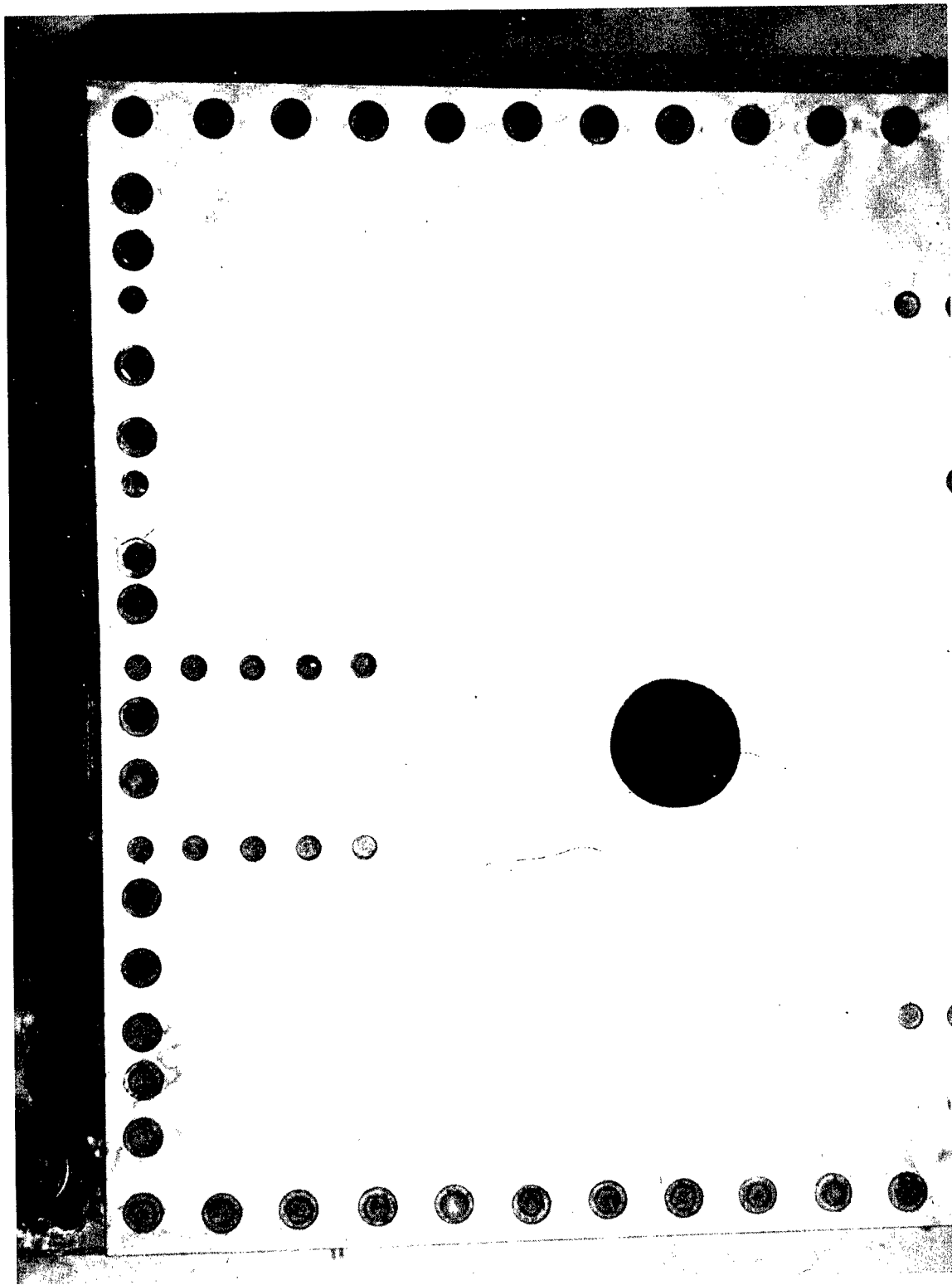


Figure 13. Photostress Evaluation, Box Beam Number 1.
View Showing Isochromatics Around Circular Cut-out

DOOR DOUBLER AT $Y = + 23.0$ ———— SEE FIGURE 4
 DOOR DOUBLER AT $Y = + 4.3$ - - - - - SEE FIGURE 4

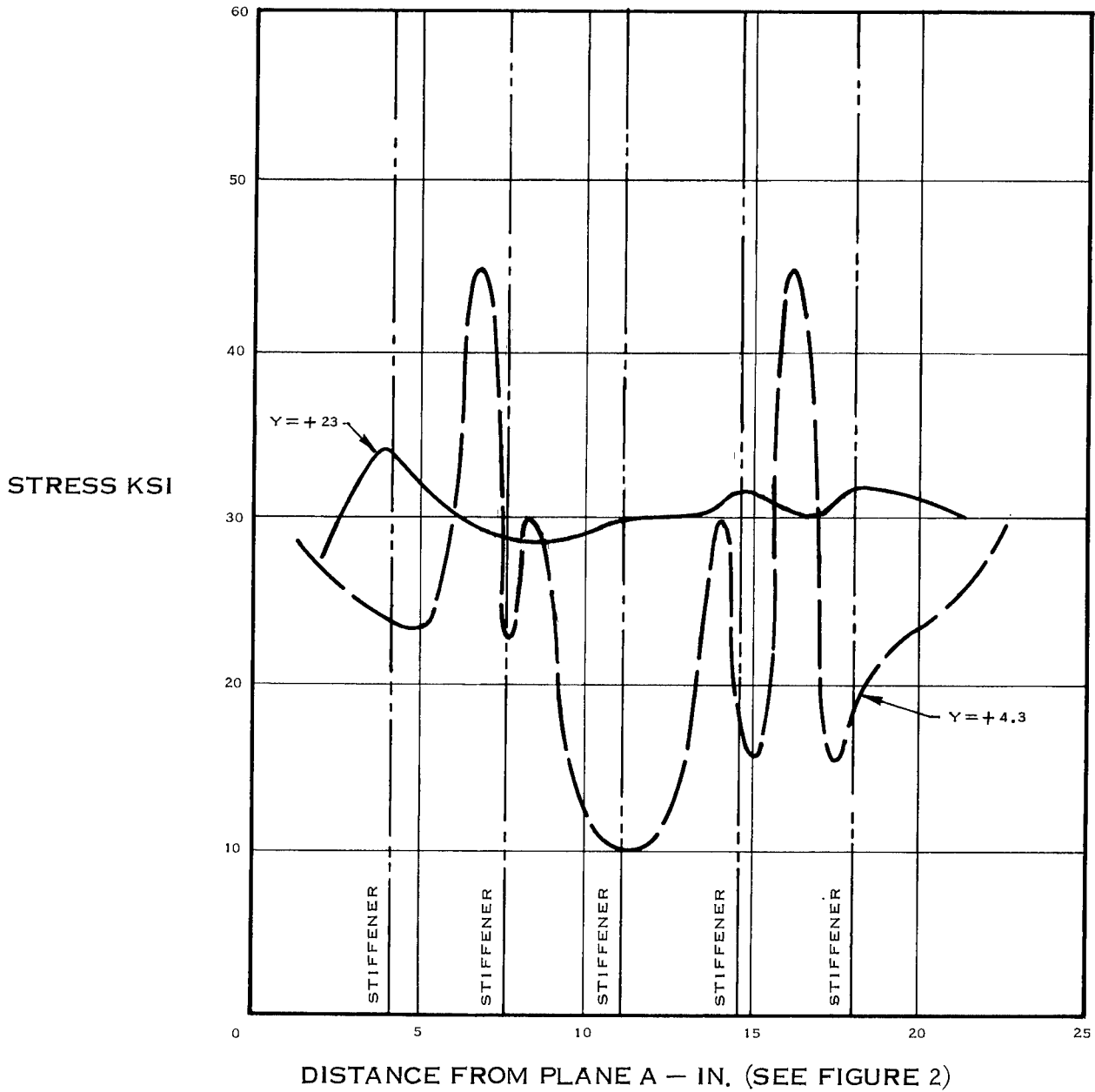


Figure 14. Sketch Showing Chordwise Stress Variation at Critical Sections

DOUBLER AT CUT-OUT $Y = -8.6$ ——— SEE FIGURE 6
 CENTER OF CUT-OUT $Y = -13.55$ ——— SEE FIGURE 6

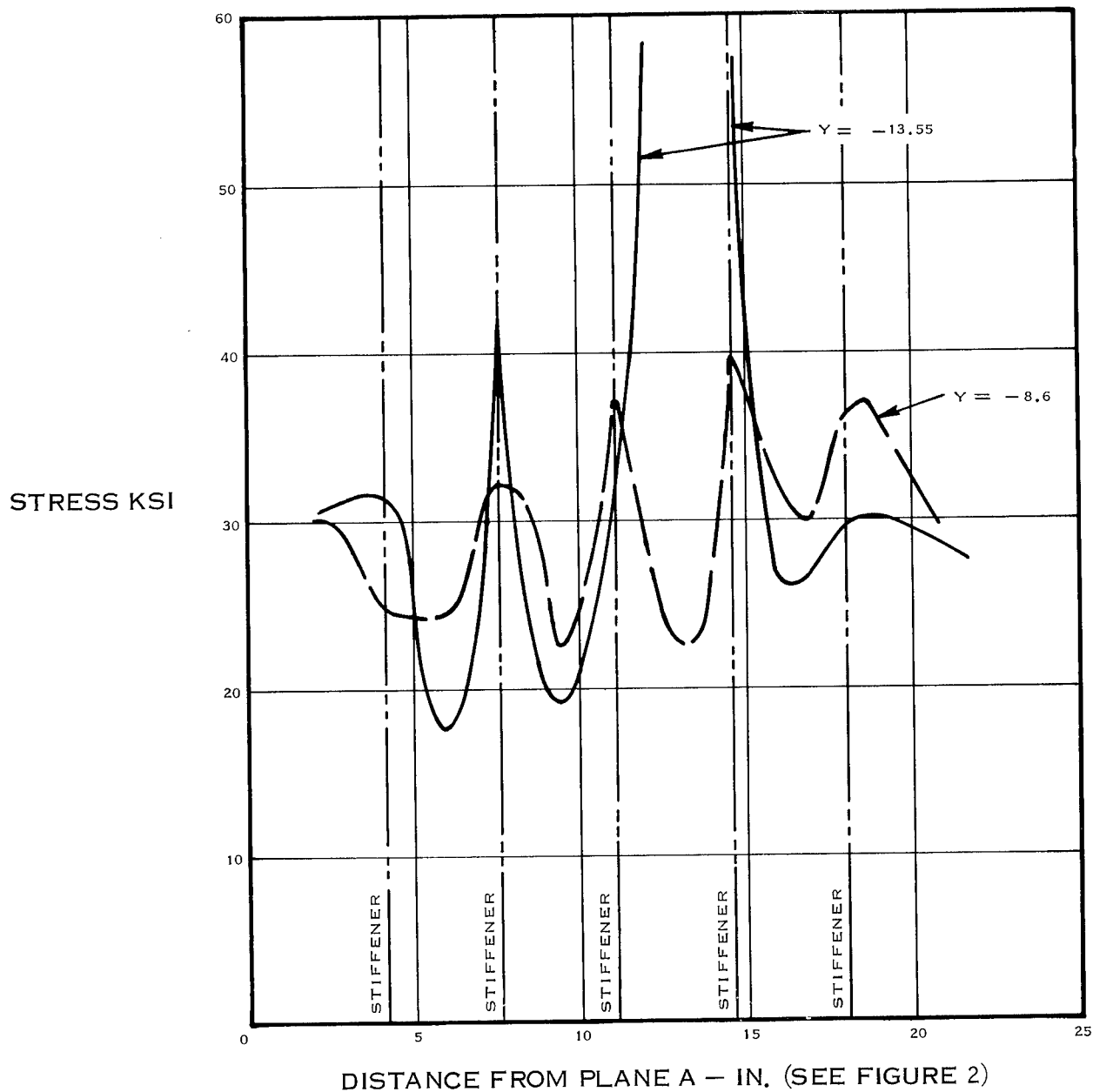
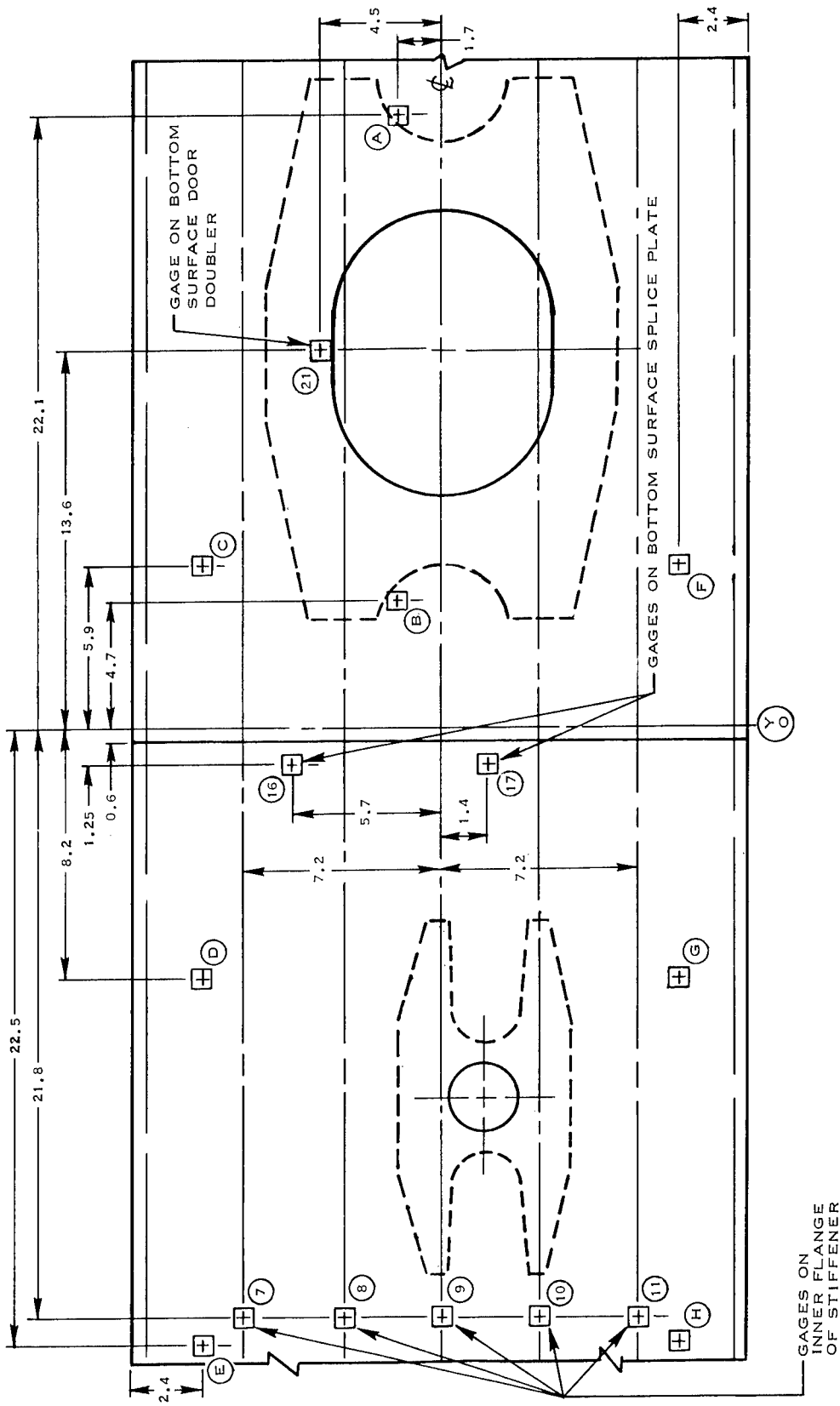


Figure 14. Sketch Showing Chordwise Stress Variation of Critical Sections (Concluded)



NOTE: ALL GAGES ON OUTSIDE OF TEST SKIN
UNLESS OTHERWISE NOTED

Figure 15. Sketch Showing Strain Gage Locations

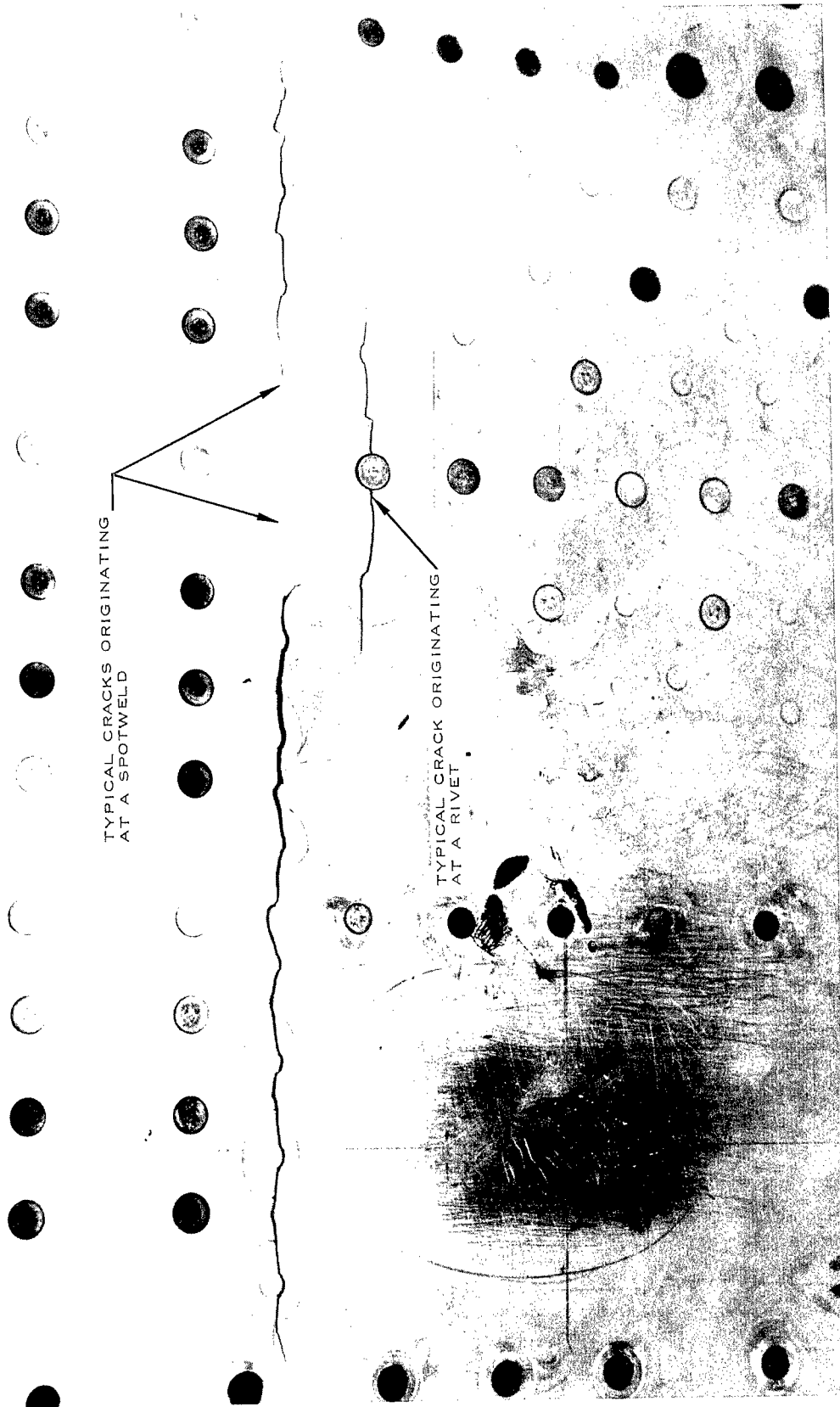
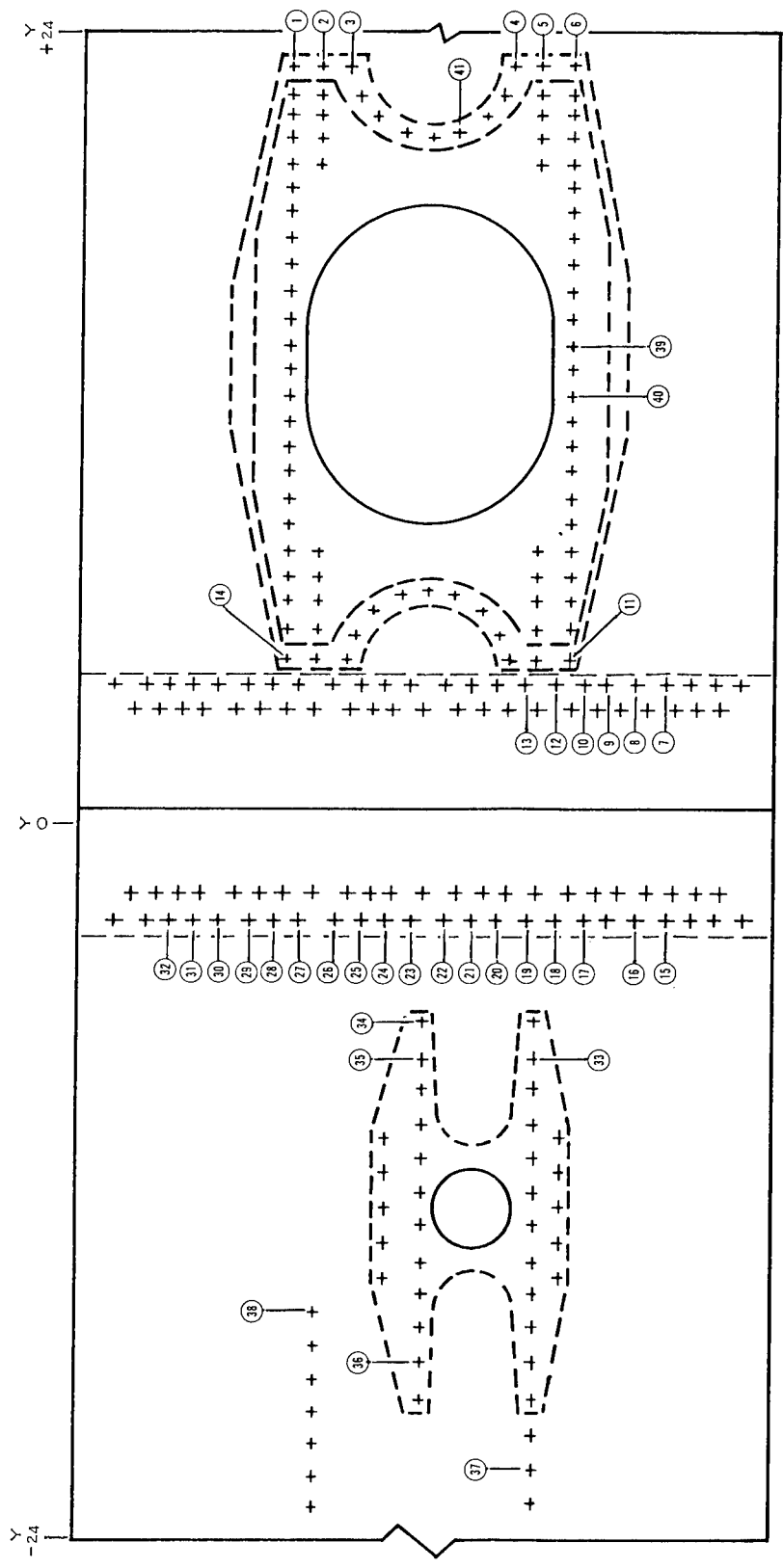
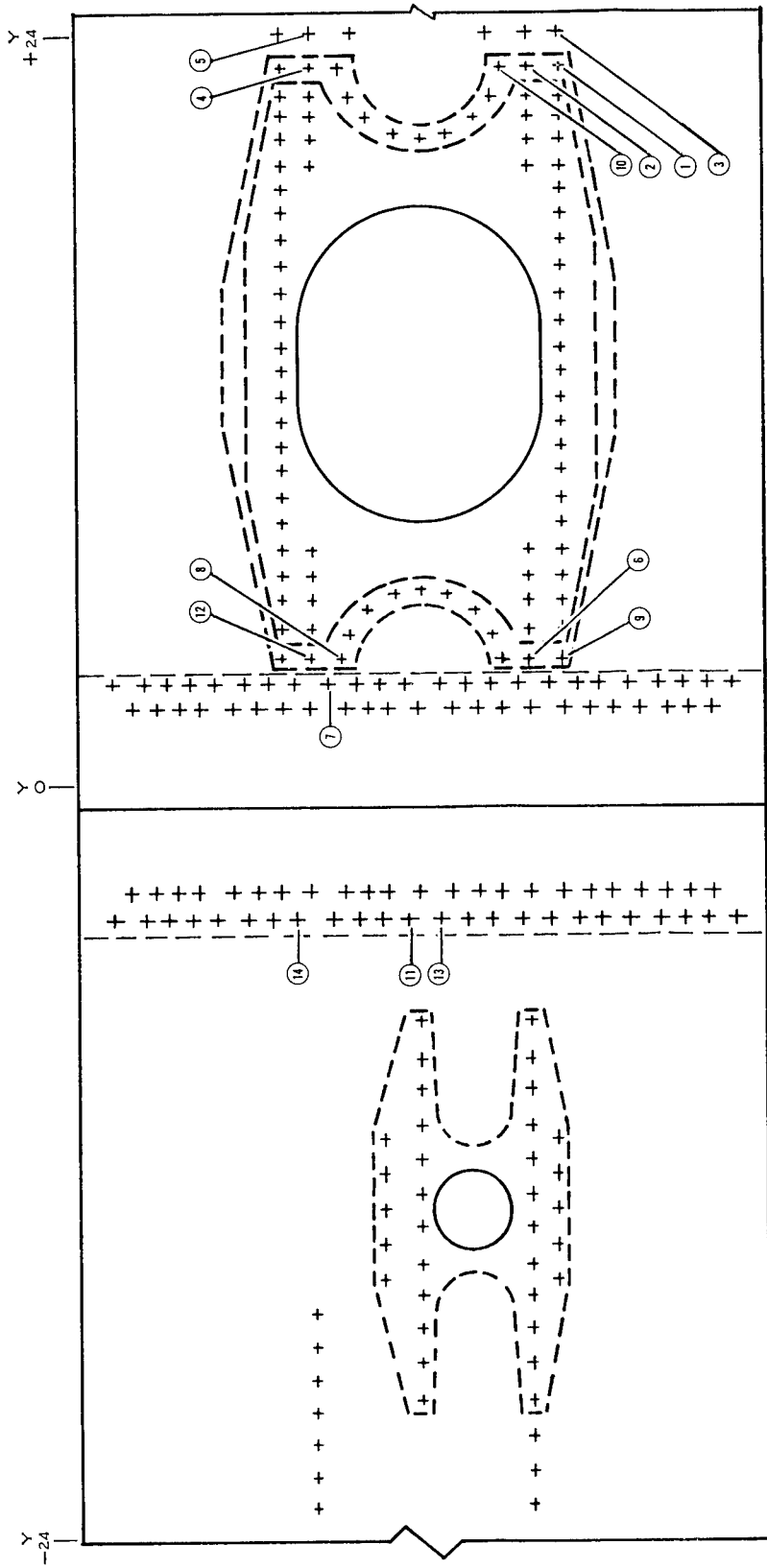


Figure 16. Photo Showing Typical Cracks Around Rivets and Spotwelds. Number 4 Test Skin



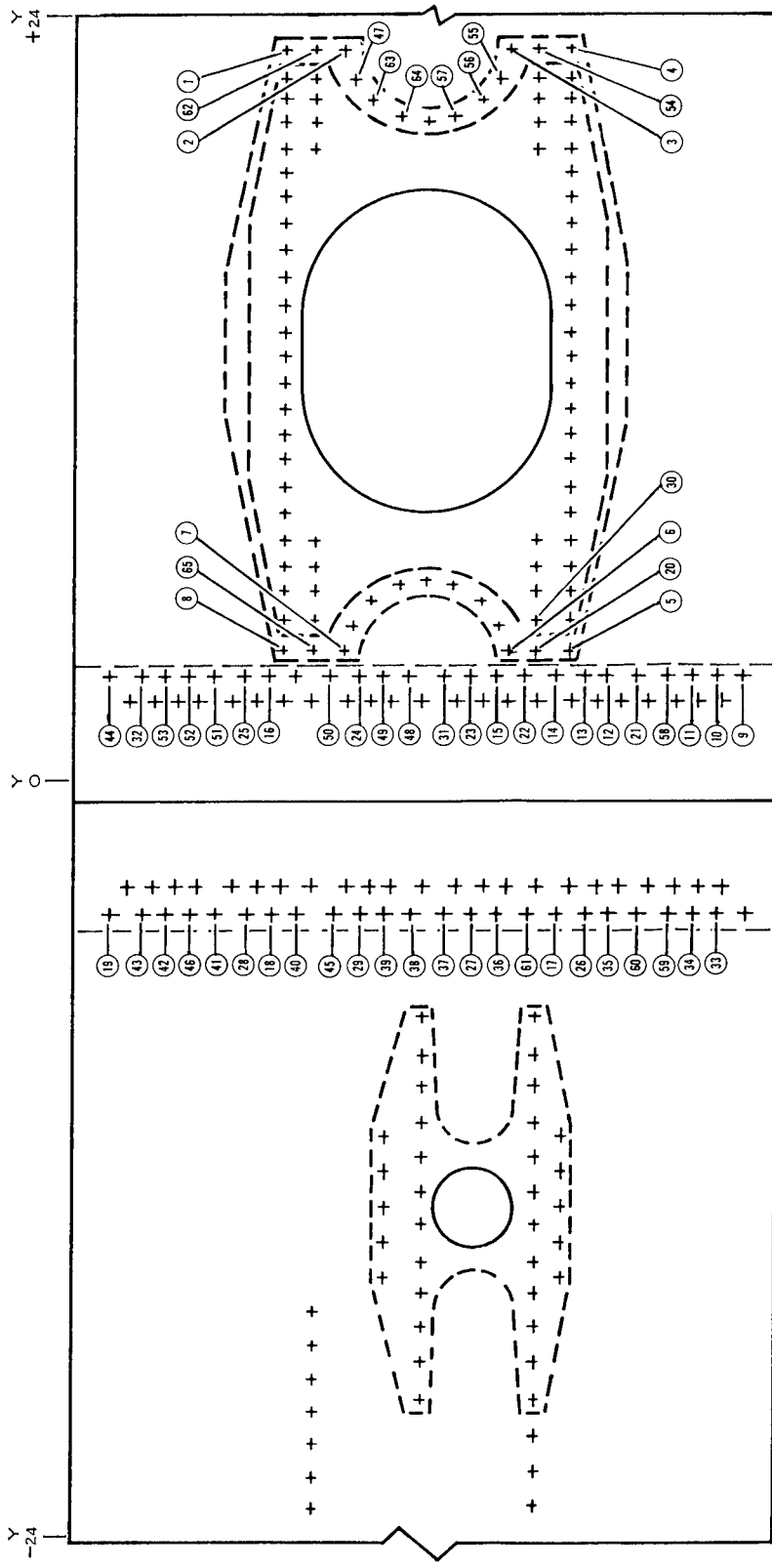
CONSTANT AMPLITUDE. R. T., $S_{MAX} = +25$ KSI, $S_{MIN} = -12.5$ KSI

Figure 17. Fatigue Crack Location in Spotweld Test Specimen Number 2



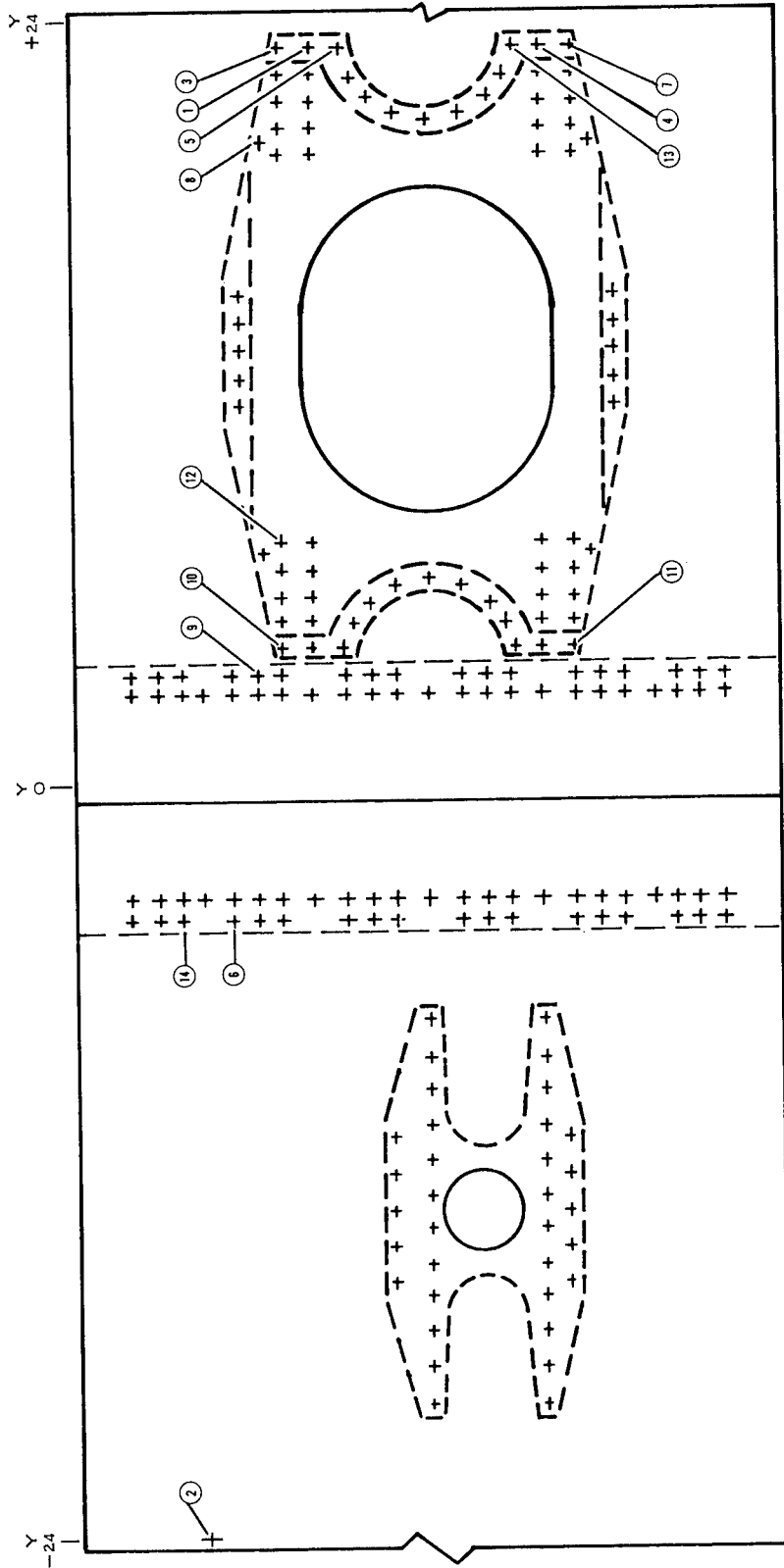
CONSTANT AMPLITUDE, 550⁰ F, $S_{MAX} = +41.25$ KSI, $S_{MIN} = +28.75$ KSI

Figure 18. Fatigue Crack Locations in Spotwelded Test Specimen Number 3



SPECTRUM TEST, SIGD=+25 KSI

Figure 19. Fatigue Crack Locations in Spotwelded Test Specimen Number 4



CONSTANT AMPLITUDE, R. T., $S_{MAX} = +25$ KSI, $S_{MIN} = -12.5$ KSI

Figure 20. Fatigue Crack Locations in Riveted Test Specimen Number 5

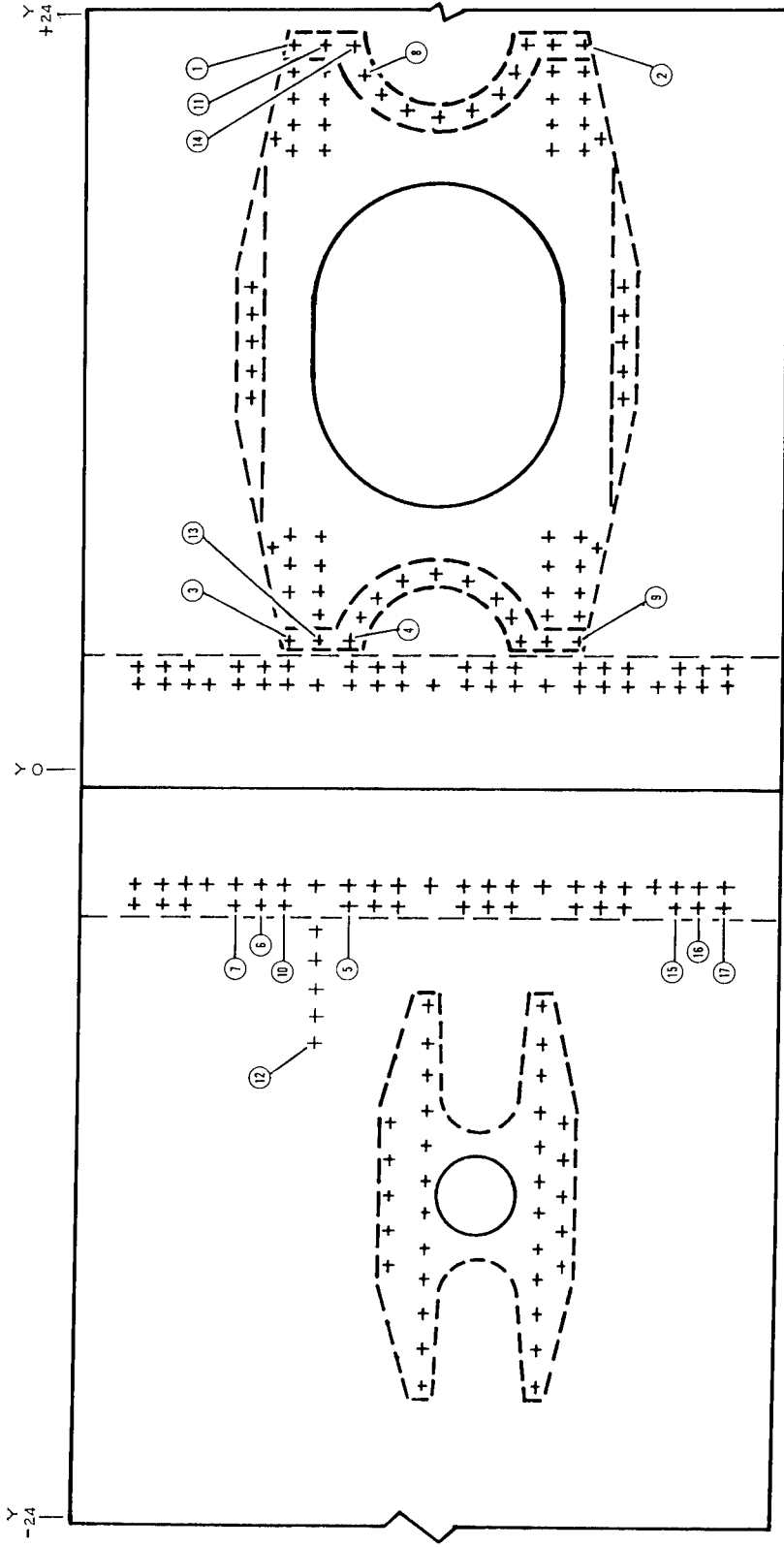
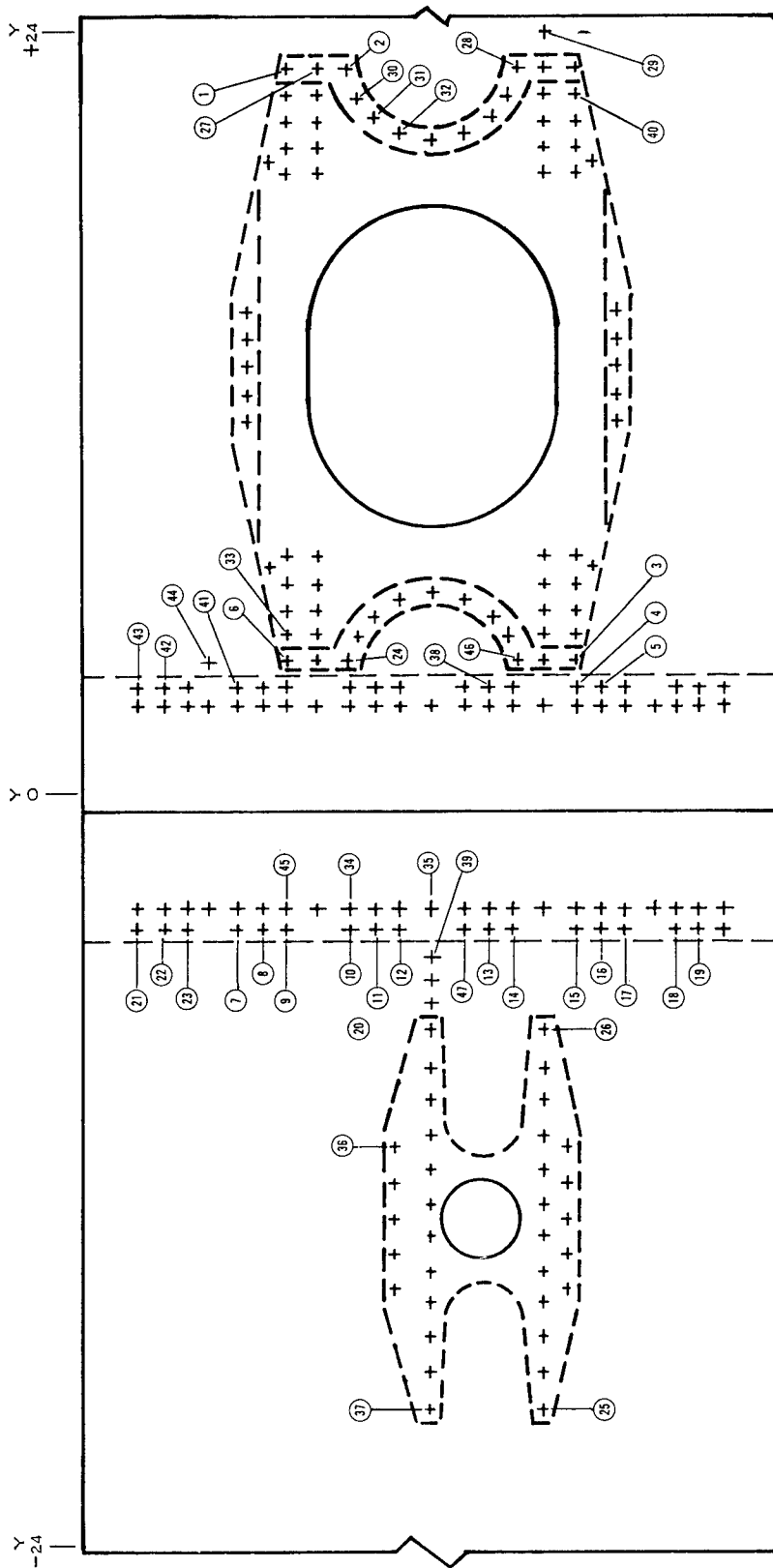
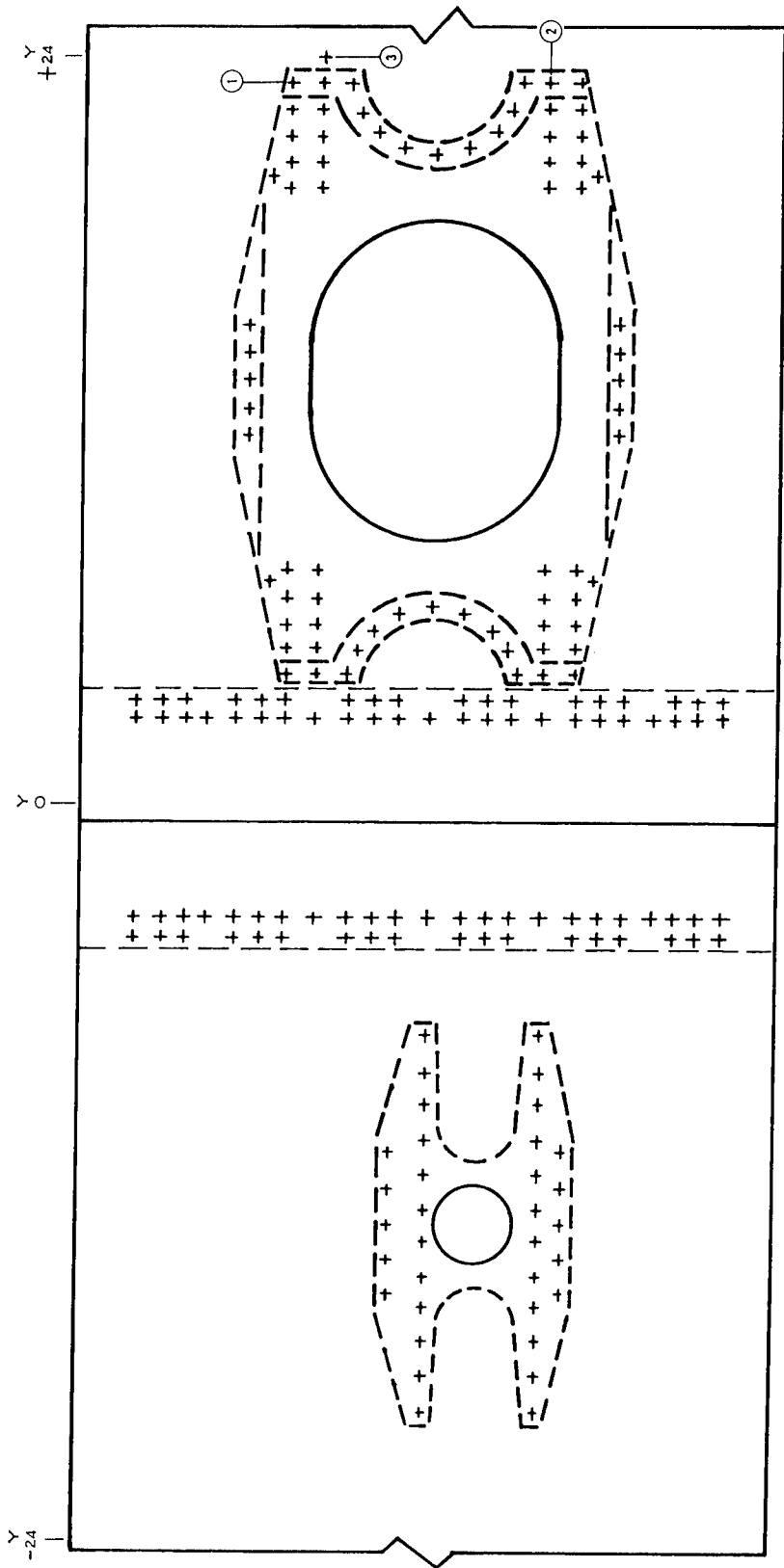


Figure 21. Fatigue Crack Locations in Riveted Test Specimen Number 6



CONSTANT AMPLITUDE, 550⁰ F, S_{MAX}=+41.25 KSI, S_{MIN}=+28.75 KSI

Figure 22. Fatigue Crack Locations in Riveted Test Specimen Number 7



SPECTRUM TEST, SIGD=+25 KSI

Figure 23. Fatigue Crack Locations in Riveted Test Specimen Number 8

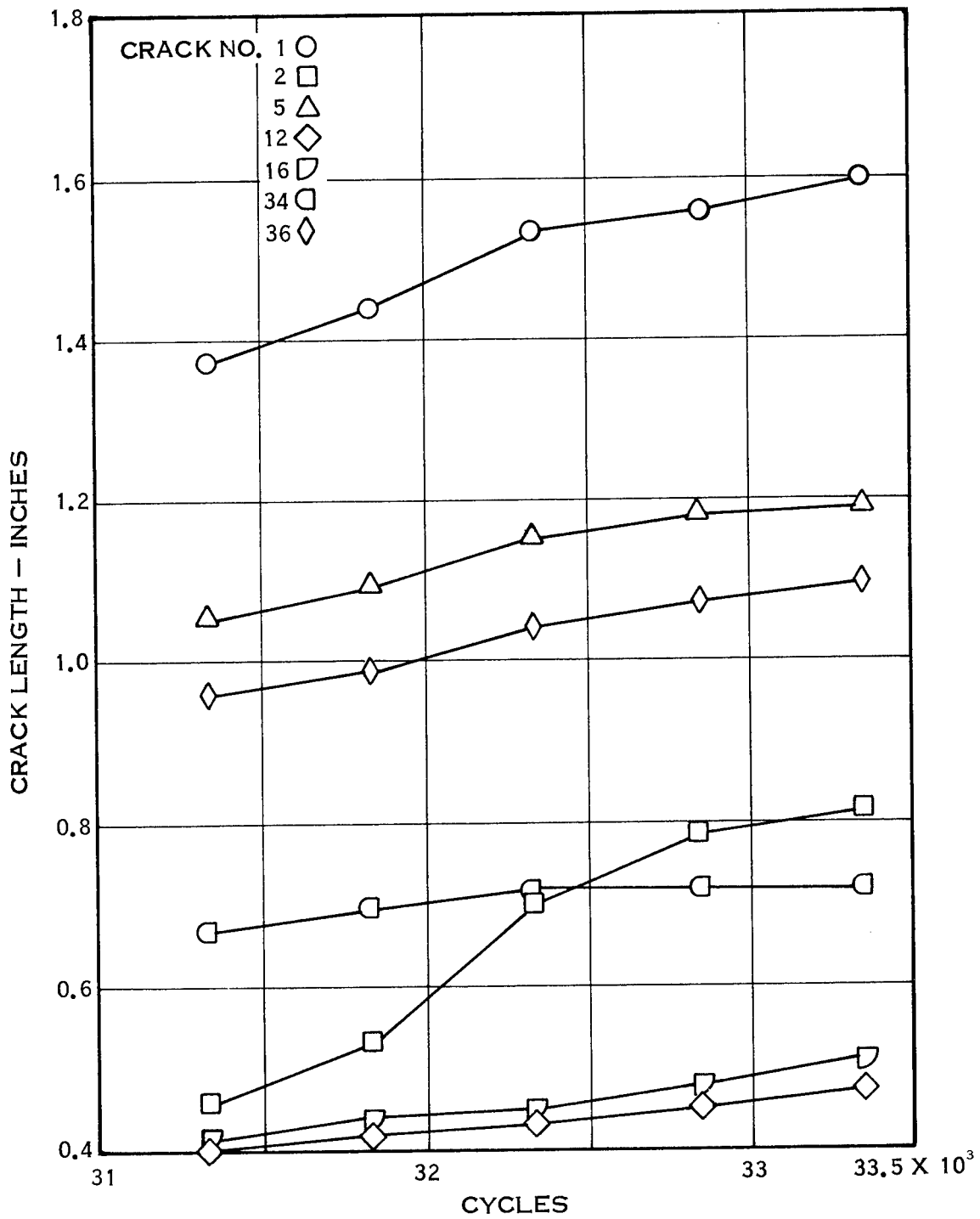


Figure 24. Crack Propagation Curves for Selected Cracks, Test Specimen Number 2

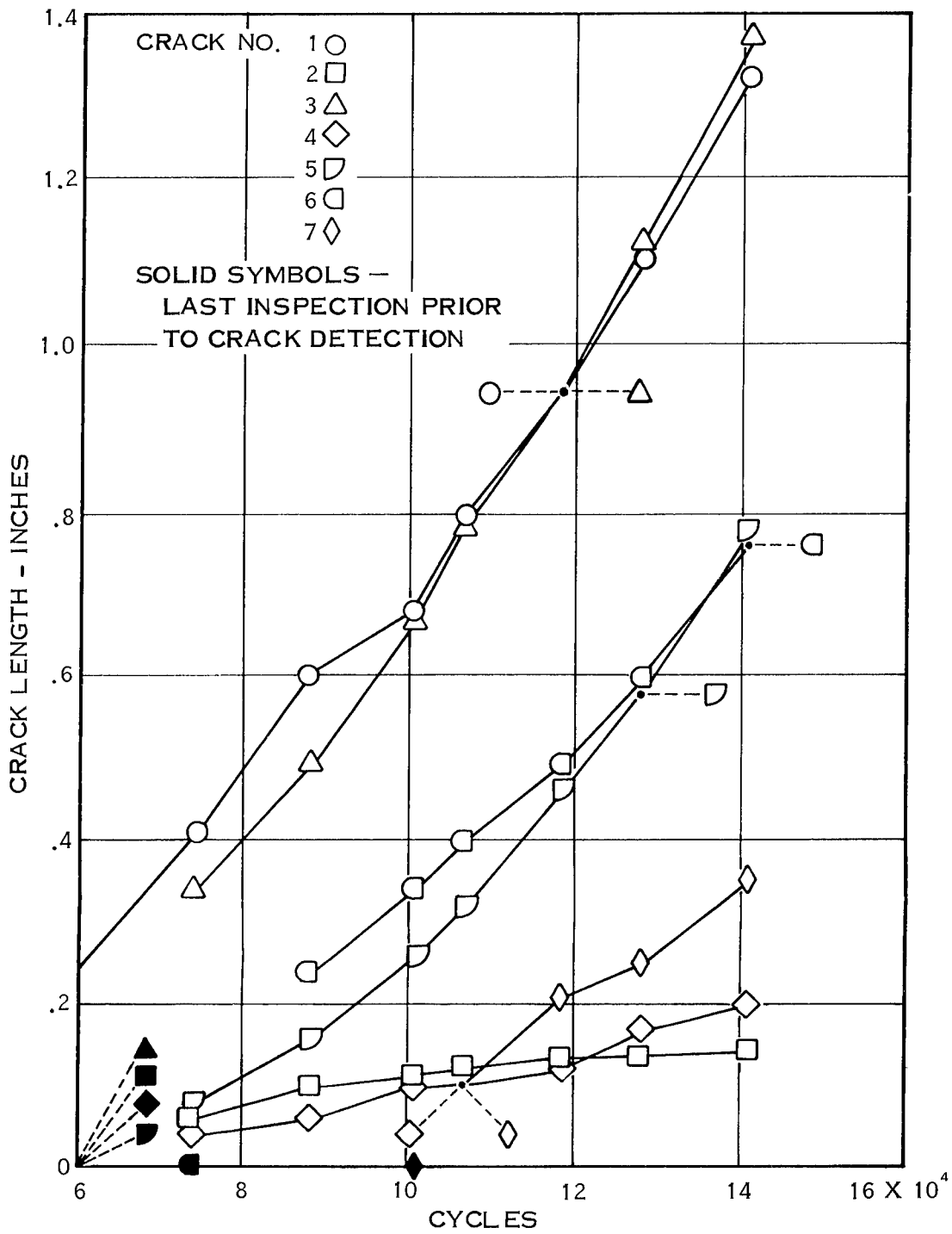


Figure 25. Crack Propagation Curves for Test Specimen Number 3

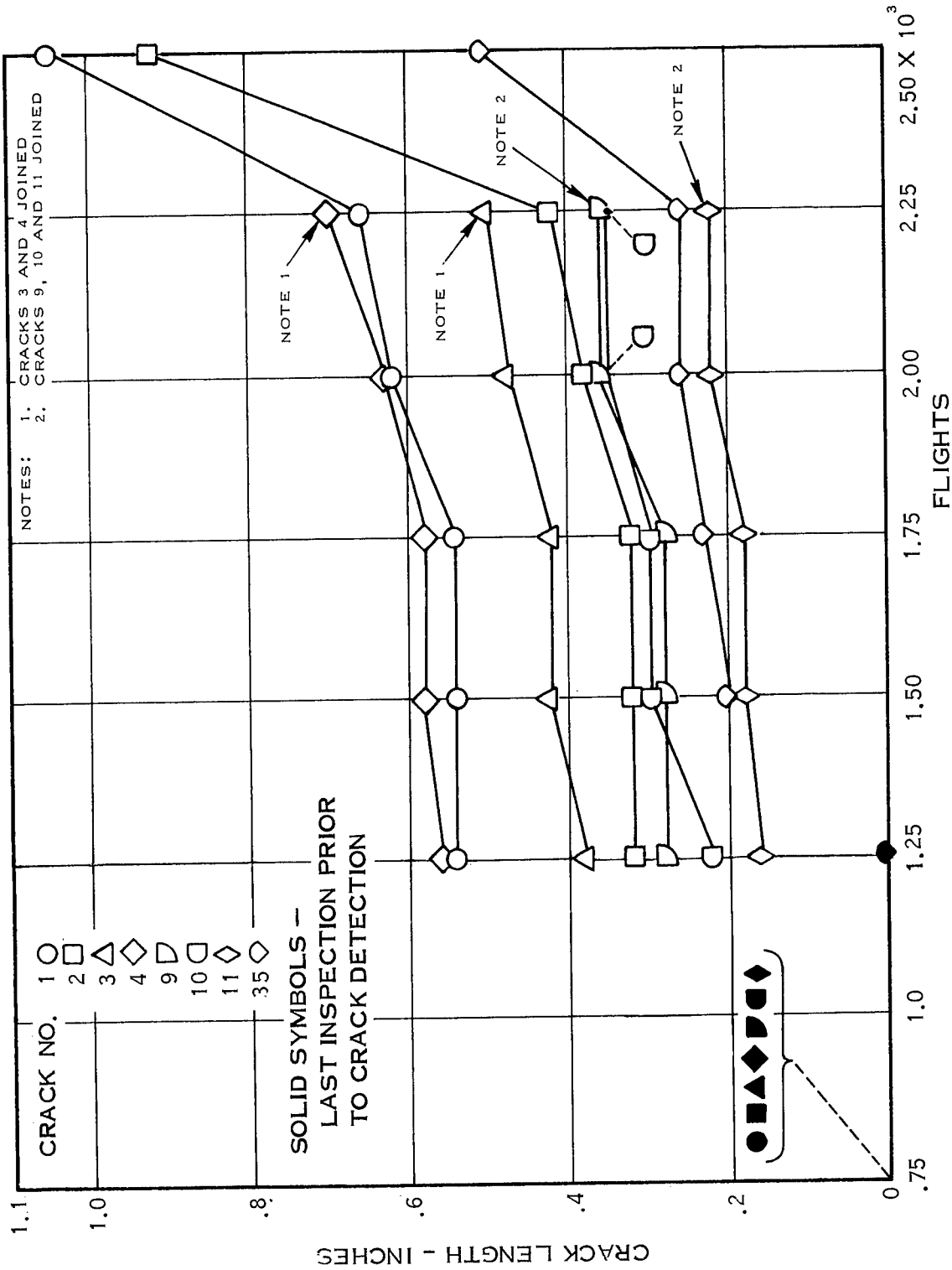


Figure 26. Crack Propagation Curves for Selected Cracks, Test Specimen Number 4

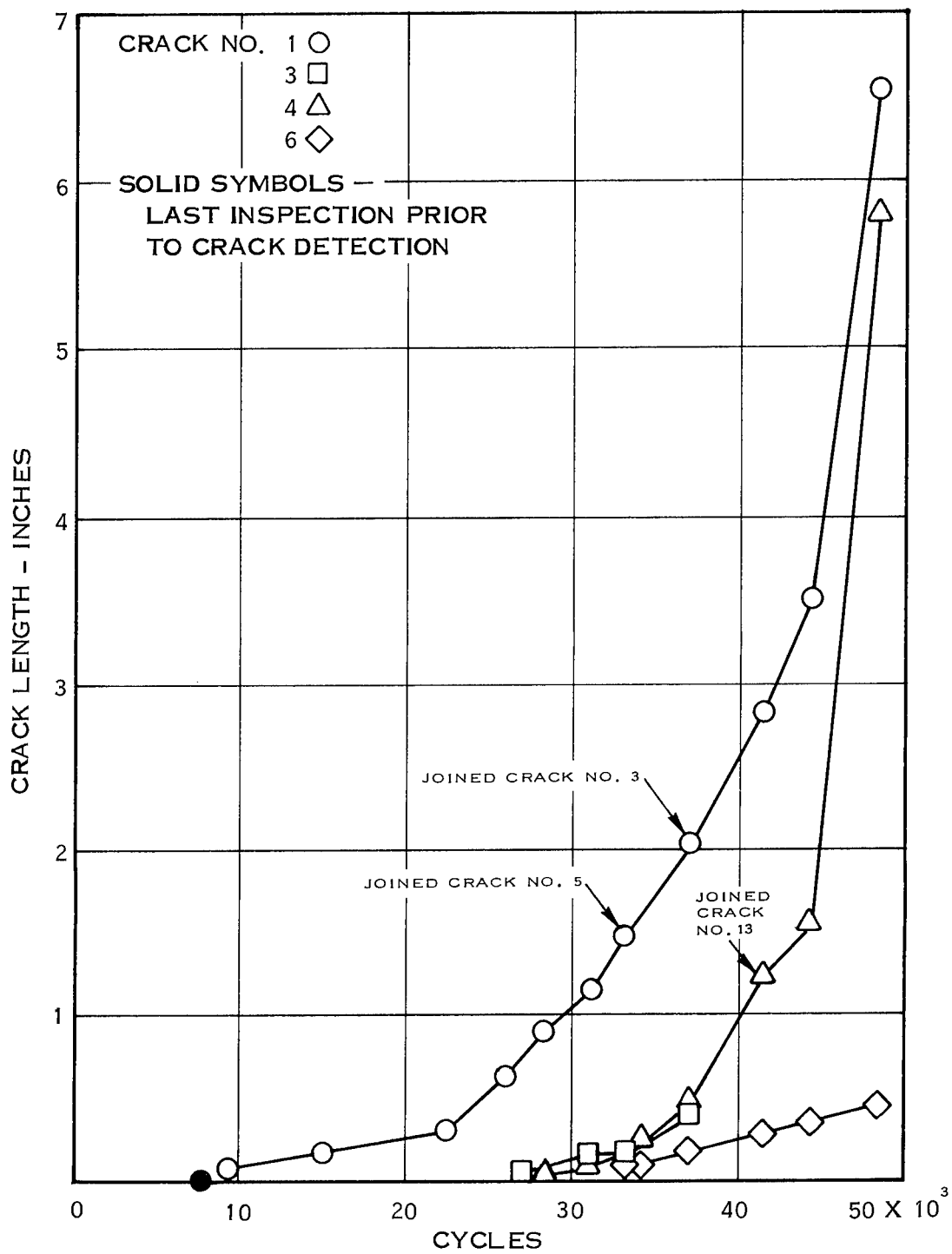


Figure 27. Crack Propagation Curves for Selected Cracks, Test Specimen Number 5

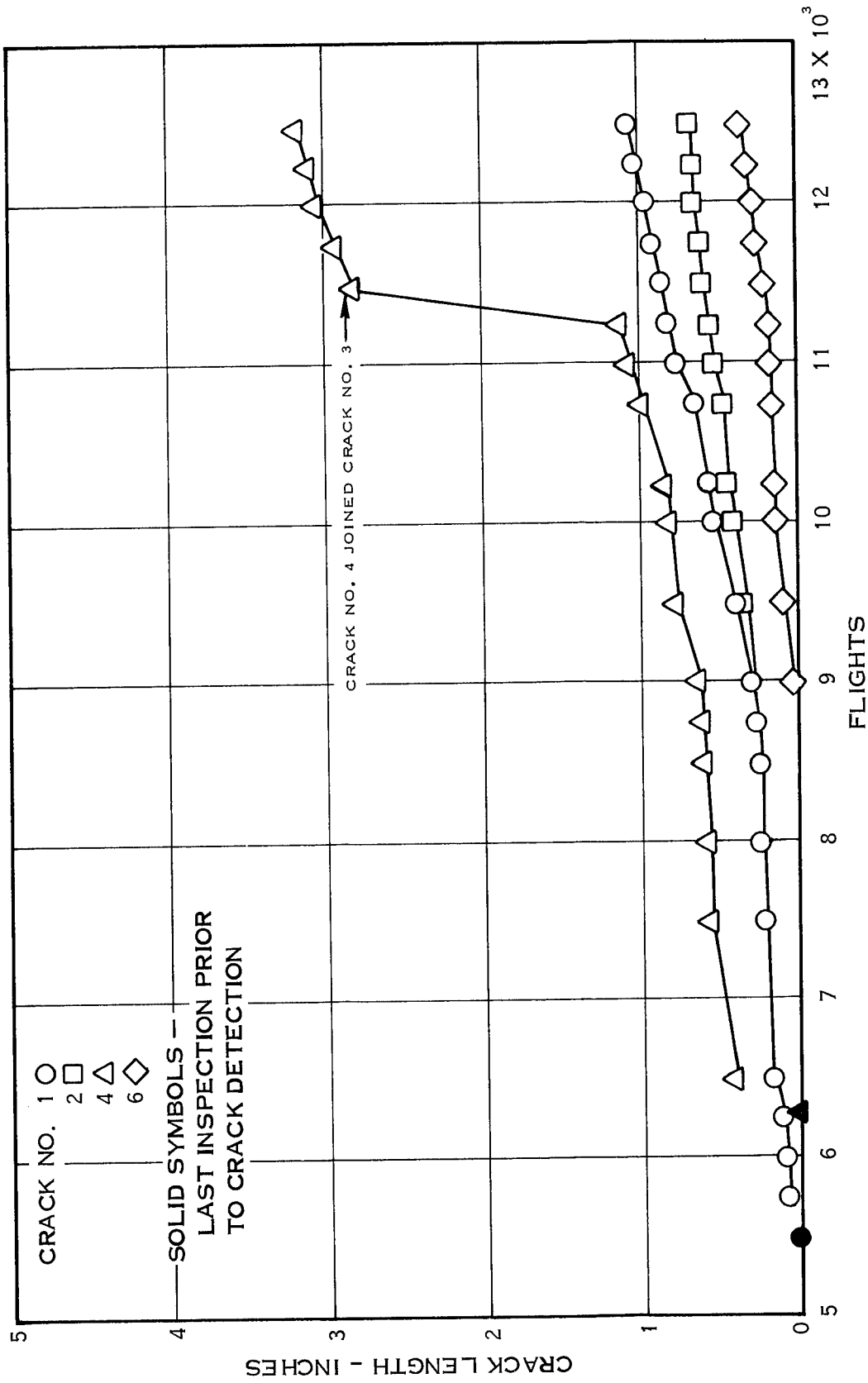


Figure 28. Crack Propagation Curves for Selected Cracks, Test Specimen Number 6

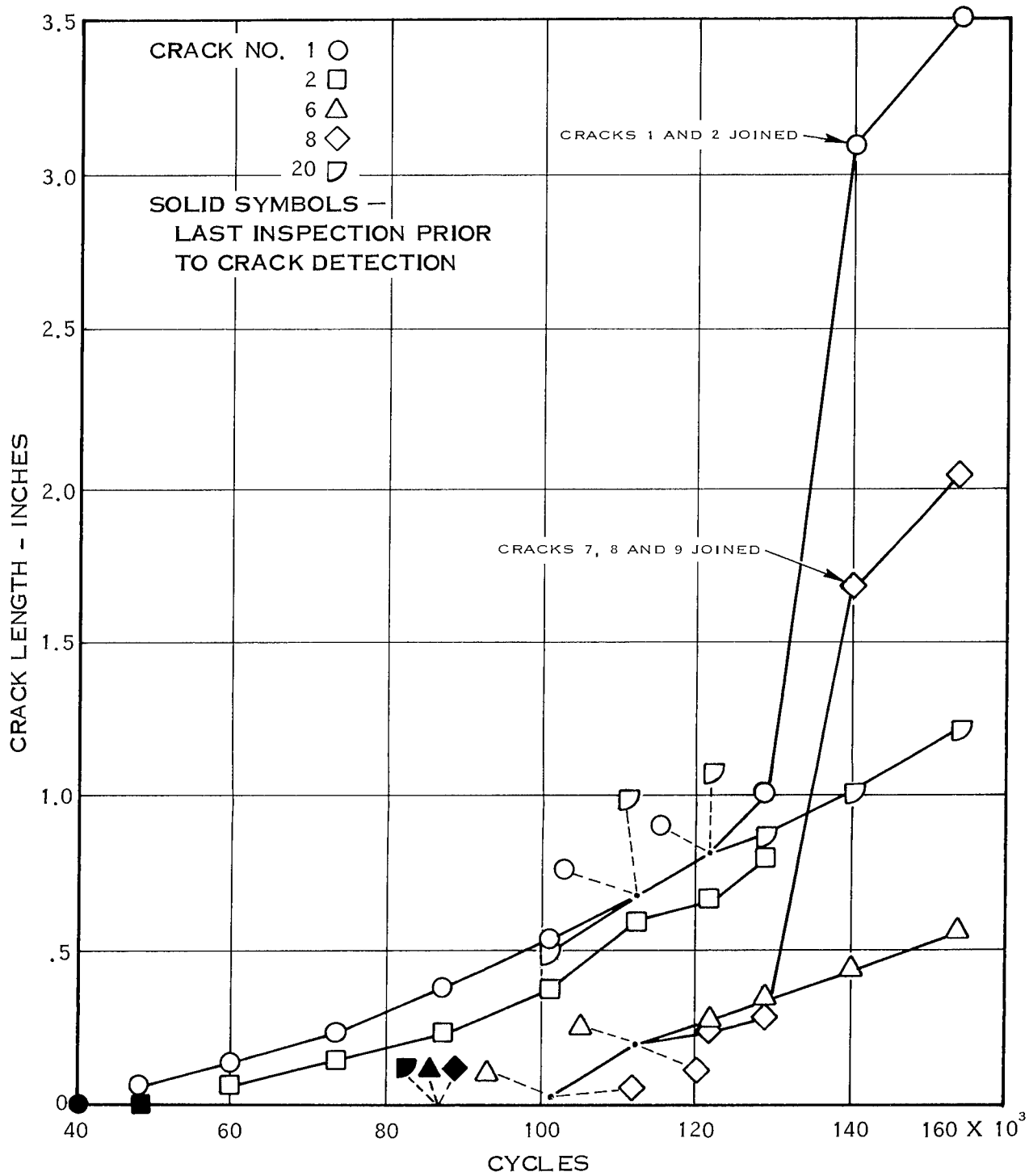


Figure 29. Crack Propagation Curves for Selected Cracks, Test Specimen Number 7

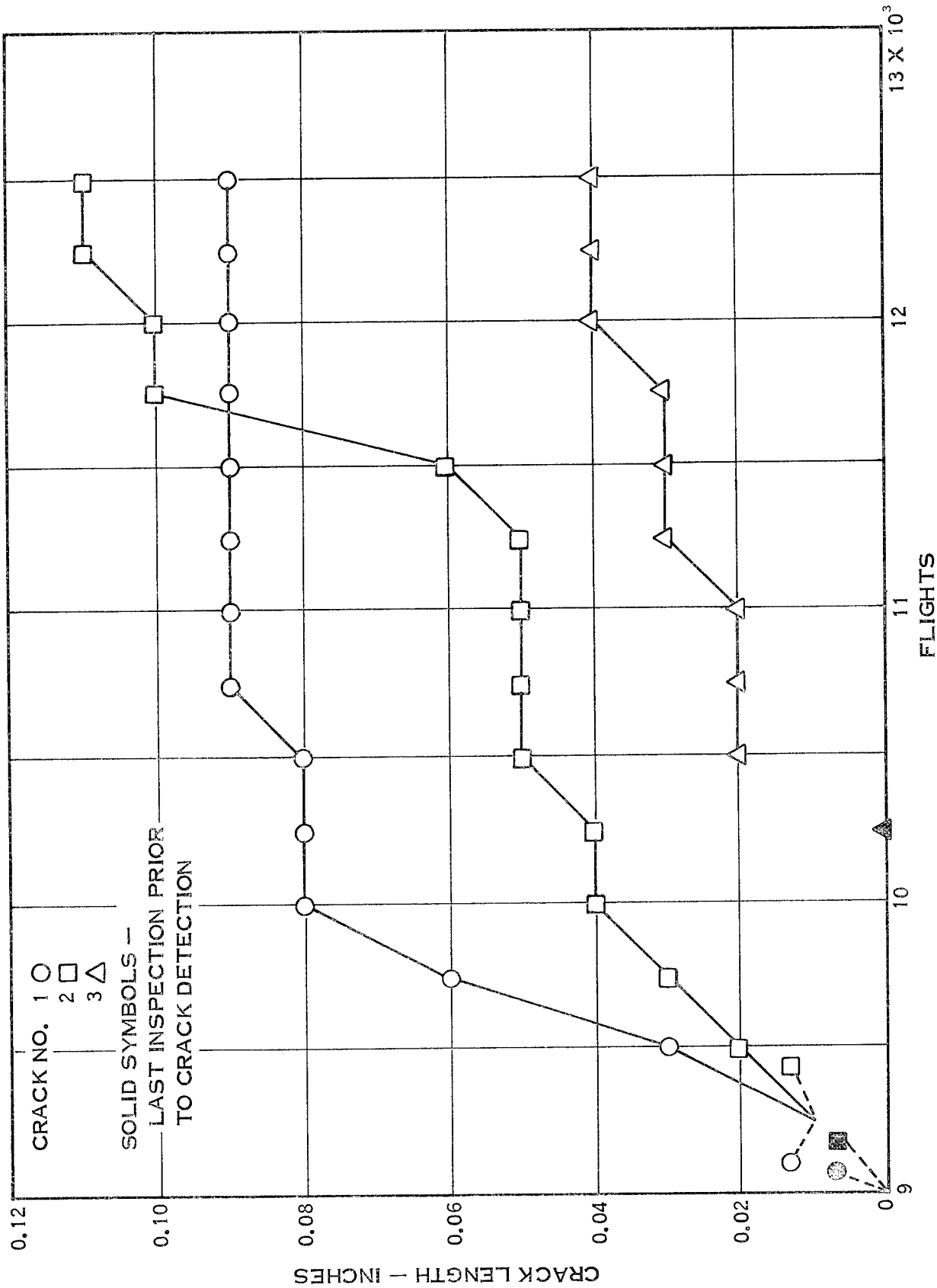
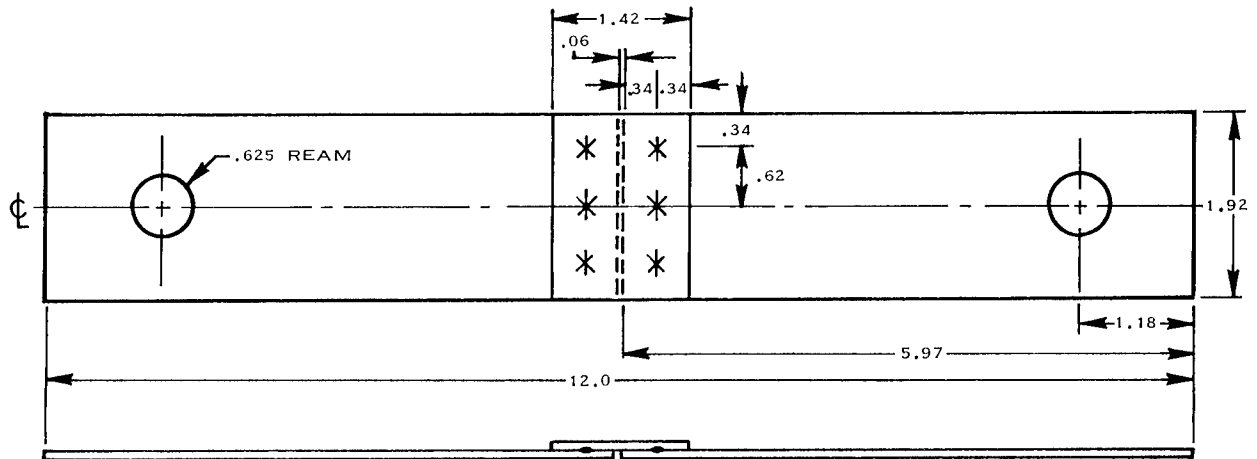
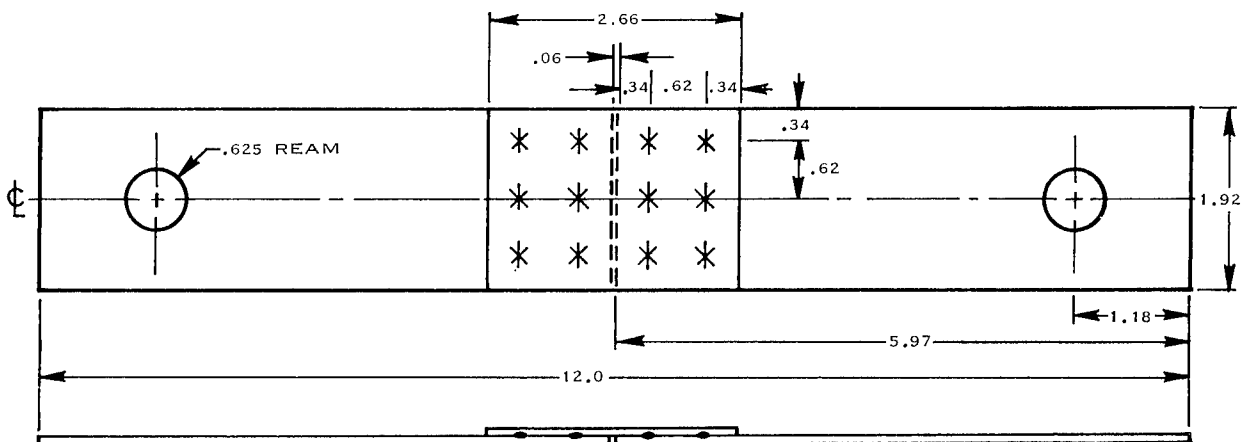


Figure 30. Crack Propagation Curves for All Cracks, Test Specimen Number 8



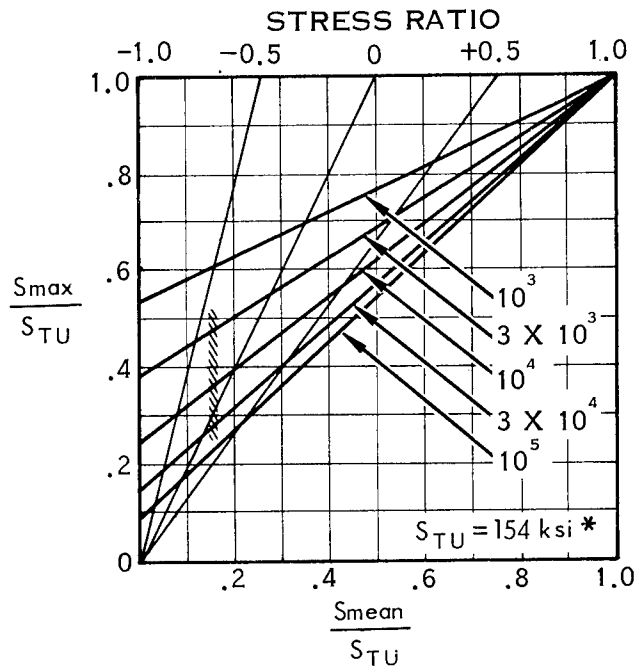
TYPE 2 - LOAD CARRYING SPOTWELD SPECIMEN



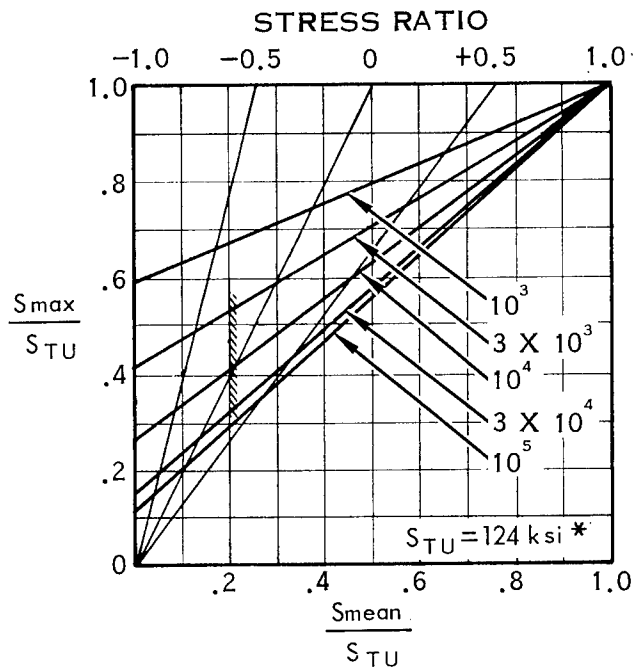
TYPE 3 - LOAD CARRYING SPOTWELD SPECIMEN

- NOTES: 1. All Material 0.050 tnom - Ti - 8Al - 1 Mo - IV
 2. ϕ Holes and ϕ Specimen to Coincide Within 0.005
 3. All Other Tolerances ± 0.01

Figure 31. Specimen Configuration - Load Carrying Spotwelds



(A) ROOM TEMPERATURE



(B) 550°F

NOTE: Test data enclosed in shaded areas

* PARENT METAL STRENGTH

Figure 32. Modified Goodman Diagrams, Ti-8Al-1Mo-IV Triplex Annealed: Load Carrying Spotwelds

"The aeronautical and space activities of the United States shall be conducted so as to contribute . . . to the expansion of human knowledge of phenomena in the atmosphere and space. The Administration shall provide for the widest practicable and appropriate dissemination of information concerning its activities and the results thereof."

—NATIONAL AERONAUTICS AND SPACE ACT OF 1958

NASA SCIENTIFIC AND TECHNICAL PUBLICATIONS

TECHNICAL REPORTS: Scientific and technical information considered important, complete, and a lasting contribution to existing knowledge.

TECHNICAL NOTES: Information less broad in scope but nevertheless of importance as a contribution to existing knowledge.

TECHNICAL MEMORANDUMS: Information receiving limited distribution because of preliminary data, security classification, or other reasons.

CONTRACTOR REPORTS: Technical information generated in connection with a NASA contract or grant and released under NASA auspices.

TECHNICAL TRANSLATIONS: Information published in a foreign language considered to merit NASA distribution in English.

TECHNICAL REPRINTS: Information derived from NASA activities and initially published in the form of journal articles.

SPECIAL PUBLICATIONS: Information derived from or of value to NASA activities but not necessarily reporting the results of individual NASA-programmed scientific efforts. Publications include conference proceedings, monographs, data compilations, handbooks, sourcebooks, and special bibliographies.

Details on the availability of these publications may be obtained from:

SCIENTIFIC AND TECHNICAL INFORMATION DIVISION
NATIONAL AERONAUTICS AND SPACE ADMINISTRATION

Washington, D.C. 20546